The polychromatic T-matrix

Maxim Vavilin [a],[*], Ivan Fernandez-Corbaton [b]

[a] *Institute of Theoretical Solid State Physics, Karlsruhe Institute of Technology, 76128, Karlsruhe, Germany*
[b] *Institute of Nanotechnology, Karlsruhe Institute of Technology, 76021, Karlsruhe, Germany*

ARTICLE INFO

ABSTRACT

The T-matrix is a powerful tool that provides the complete description of the linear interaction between the electromagnetic field and a given object. In here, we generalize the usual monochromatic formalism to the case of polychromatic field-matter interaction. The group of transformations of special relativity provides the guidance for building the new formalism, which is inherently polychromatic. The polychromatic T-matrix affords the direct treatment of the interaction of electromagnetic pulses with objects, even when the objects move at constant relativistic speeds.

1. Introduction

Understanding and engineering the interaction between electromagnetic radiation and matter has been, is, and will be crucial for our scientific and technological development. These endeavors benefit from accurate an efficient theoretical and numerical tools of wide applicability. The T-matrix is a particularly useful formalism for the study of light-matter interactions featuring such beneficial properties. The T-matrix of an object is a linear operator that produces the field scattered by the object upon a given incident illumination. In the most common embodiment the incident field is expanded into regular multipolar fields, the scattered field is expanded into irregular outgoing multipolar fields, and the T-matrix connects the two sets of expansion coefficients. Following the seminal paper by Waterman [1], the T-matrix formalism has been established as one of the most powerful and popular techniques for computing the electromagnetic response of single and composite objects. The amount of research related to the T-matrix and its manifold applications grows at an increasing rate [2,3].

For all its outstanding properties, the T-matrix formalism has still some limitations. One important question whose theoretical details and algorithmic answers are currently under intense study [4–10] is the validity of the expansion of the scattered fields outside the object, but inside the smallest sphere circumscribing the object. Such question compromises the computation of the joint T-matrix of two objects that invade each others smallest circumscribing spheres. In here, we address another important limitation. The T-matrix formalism is monochromatic at its core, that is, it has been defined and developed systematically assuming that the illuminating fields are monochromatic, with time dependence $\exp(-i\omega_0 t)$ for some fixed frequency ω_0. It

is clear that the linearity of Maxwell equations permits the computation of the response of an object to an incident polychromatic field by superposing the responses to many monochromatic fields with different frequencies. Yet, as far as we know, a systematic development of the polychromatic T-matrix does not exist, which in particular leaves out the direct treatment of the interaction of objects with light pulses. The practical significance of such interactions is already well recognized, including applications such as particle size and refractive index measurements [11], pulsed optical tweezers [12], and reversion of matter magnetization [13]. Other cases where a robust polychromatic T-matrix formalism will be beneficial are linear processes that change the frequency of light. One example is the illumination of objects moving at constant speeds. While the source may be approximately monochromatic in its frame, new frequencies will appear after considering the light in the reference frame of the object. The problem is readily solved if the T-matrix in the rest frame of the object can be transformed with the appropriate Lorentz boost. Raman scattering is another example where the energy of internal vibrations in the object is added to or subtracted from the incident frequency, while the response is still linear from the point of view of the illumination.

We will use an approach to the T-matrix that is not in the main stream of T-matrix research, but that has already shown its value. The T-matrix can be approached from the perspective of group theory, that is, the study of symmetry transformations of physical systems [14]. Of special importance for the T-matrix is the concept of irreducible representations of a group of transformations, which can be understood as elementary components of e.g. an operator or a physical field,

* Corresponding author.
E-mail address: maxim.vavilin@kit.edu (M. Vavilin).

Nomenclature

ϵ_0	Vacuum permittivity
$\hbar$	Reduced Planck constant
λ	Helicity
ξ	Rapidity
c	Speed of light in vacuum
$C_{j_1 m_1; j_2 m_2}^{j_3 m_3}$	Clebsch–Gordan coefficient
$D_{mn}^j(\alpha, \beta, \gamma)$	Wigner matrix
$d_{mn}^j(\beta)$	Small Wigner matrix
$x^\mu y_\mu$	Scalar product in $(- + + +)$ Minkowski metric
$\begin{pmatrix} j_1 & j_2 & j_3 \\ m_1 & m_2 & m_3 \end{pmatrix}$	Wigner 3j-symbol

that transform in distinct ways under the transformations belonging to a given group, and that do not mix with each other upon such transformations. Starting from the T-matrix formalism that Waterman had developed for a single object [1], Peterson and Ström extended it to multiple objects with the help of group theory [15]. They showed that the monochromatic T-matrix transforms according to the 3D Euclidean group, which consists of spatial translations and rotations, and exploited the transformation properties of the irreducible representations of such group for conveniently formulating the translations and rotations of individual T-matrices that are needed for computing the T-matrix of a composite object. The connection between the monochromatic T-matrix and the 3D Euclidean group is well illustrated by the fact that the translation theorems for vector spherical harmonics can be derived within the context of group theory [14, Secs. 8.6 and 9.8].

The 3D Euclidean group is not sufficient for treating polychromatic electromagnetic fields. Wigner showed in a landmark paper [16] that physical fields describing elementary particles such as electrons and photons transform under the Poincaré group, which consist of the 3D Euclidean group plus time translations and Lorentz boosts, also known as Lorentz transformations, or changes of inertial reference frame. Lorentz boosts change the frequency content of the field, as exemplified by the Doppler effect, which makes a monochromatic treatment impossible. The Poincaré group is the group of transformations of special relativity, and its relevance in electromagnetism can be appreciated in the decomposition of the electromagnetic field in irreducible parts [17], and in the formulation of a scalar product [18] between two given electromagnetic fields whose result is invariant under all the transformations of the Poincaré group. Such scalar product enables one to use the tools of Hilbert spaces in electromagnetism and, in particular, allows one to systematically compute fundamental quantities such as energy and momentum contained in a given electromagnetic field [19, §9, Chap. 3]. Combining the scalar product with the S-matrix operator, one obtains a unified theory of conservation laws in light-matter interactions [20]. The S-matrix is a linear operator that maps irregular incoming fields to irregular outgoing fields, and that is numerically related to the T-matrix in a bijective and straightforward manner.

In this article, we extend the T-matrix formalism to the polychromatic setting by following the guidance provided by the representation of the Poincaré group of transformations in the Hilbert space of solutions of Maxwell equations. The formalism developed with the help of such algebraic structures and methods is inherently polychromatic, and facilitates the definitions of basis states and frequency integrals, among other aspects. The appropriate basis states and corresponding expansion coefficient functions for the fields are found by requiring that they transform unitarily according to the representations of the Poincaré group appropriate for photonic fields, as established by Wigner [16]. The requirement of unitarity is fulfilled with respect to the scalar product whose result is invariant under all the transformations of

the conformal group [18], which includes the Poincaré group. These requirements led us to modify the usual definitions of plane waves and multipolar fields. Importantly, we show that the irregular incoming and outgoing multipolar fields transform under Lorentz boost as the regular multipolar fields, a new result that is needed for building the polychromatic T-matrix formalism. As an example, we derive within our theory the relativistic transformation law that can convert the T-matrix of a stationary object into that of the object moving with a constant speed. This technique can be applied to any object described by the T-matrix, in contrast to previous approaches, which were confined to dealing with the relativistic motion of spherical objects [21,22]. Since the polychromatic domain can represent the linear dependence between general time-dependent incident and scattered fields, the polychromatic T-matrix constitutes a new theoretical method for describing time-dependent scattering, and hence complements existing approaches [23, 24].

In the rest of the article we advance towards the definition of the polychromatic T-matrix and S-matrix in the following way. First, we define the basis states that are relevant in the T-matrix and S-matrix settings. Namely, regular multipolar fields for representing incident fields and irregular multipolar fields for representing incoming, outgoing, and scattered fields. To such end, we connect in Section 2 the traditional formalism of electric and magnetic fields $\{E(r, t), B(r, t)\}$ with the formalism based on abstract kets in a Hilbert space $|f\rangle$, and then define the plane wave states so that they transform according to the massless unitary representations of the Poincaré group with well defined helicity(handedness) $\lambda = +1$, or $\lambda = -1$. The regular multipolar fields are then defined from the plane waves. Both plane waves and multipoles defined in this way feature an extra factor of k with respect to the usual definitions. Such factor ensures that both the fields and the expansion coefficients multiplying them transform unitarily under Lorentz boosts. For the case of incoming and outgoing multipolar fields, we are also led to multiply the usual definitions by a factor of $1/2$ by the notable properties of polychromatic irregular fields: namely that they vanish identically either before or after the light-matter interaction period, and are correspondingly equal to regular fields at certain time regions. We provide all the transformation properties for states and coefficients under the isometries of the Minkowski space–time: Poincaré transformations, parity, and time-reversal. The polychromatic T-matrix is defined in Section 3.1 and the polychromatic S-matrix is defined in Section 3.3. In Section 3.2 we consider the special case where the polychromatic T-matrix is diagonal in frequency, and show how to build it using monochromatic T-matrices that are computed with the usual conventions. As an exemplary application, the formalism is applied in Section 4 to the computation of the energy and linear momentum transferred from a pulse of light onto a silicon sphere.

All the numerical results contained in the paper can be reproduced with the code provided by request, together with the `treams` Python package [25,26], which is publicly available at https://github.com/tfp-photonics/treams. We note that the methodology is independent of the particular technique used for obtaining T-matrices [27–30].

2. Group theory-guided representations of electromagnetic fields

Maxwell equations in frequency domain for the electric $\tilde{E}(r, k)$ and magnetic fields $\tilde{B}(r, k)$ in vacuum and in SI units are

$$\nabla \times \tilde{E}(r, k) = ick\tilde{B}(r, k), \qquad \nabla \times \tilde{B}(r, k) = -\frac{ik}{c^2}\tilde{E}(r, k), \qquad (1)$$

$$\nabla \cdot \tilde{E}(r, k) = 0, \qquad \nabla \cdot \tilde{B}(r, k) = 0, \qquad (2)$$

where $c = 1/\sqrt{\epsilon_0 \mu_0}$ is the speed of light in vacuum and for convenience we describe frequency via the absolute value of the wavevector $k = \sqrt{k \cdot k} = |k| = \omega/c$. Since the magnetic field is completely determined by the electric field, we will focus on the latter for describing the electromagnetic field.

It is convenient to start from the complex-valued electric field in the space–time domain, defined by setting the components of negative frequency in the Fourier decomposition of the field to zero:

$$E(r, t) = \frac{1}{\sqrt{2\pi}} \int_0^\infty dk \, e^{-ikct} \, \tilde{E}(r, k), \tag{3}$$

while the real-valued electric field can be restored via

$$\mathcal{E}(r, t) = E(r, t) + E^*(r, t) = 2\Re[E(r, t)]. \tag{4}$$

2.1. Plane waves $|\mathbf{k}\lambda\rangle$

One can decompose the electric field in plane waves of right-handed circular polarization, helicity $\lambda = -1$, and of left-handed circular polarization, helicity $\lambda = 1$, using polarization vectors as defined in [31] (Sec. 1.1.4)

$$e_\lambda(\hat{k}) := -\frac{1}{\sqrt{2}} (\lambda e_\theta(\hat{k}) + i e_\phi(\hat{k})) \tag{5}$$

$$= \frac{1}{\sqrt{2}} \begin{pmatrix} -\lambda \cos\phi \cos\theta + i \sin\phi \\ -\lambda \sin\phi \cos\theta - i \cos\phi \\ \lambda \sin\theta \end{pmatrix}, \tag{6}$$

where e_θ, e_ϕ are spherical basis vectors, $\hat{k}$ is the unit vector along the direction of the wave vector, with $\theta = \arccos(k_z/|k|)$ and $\phi = \text{atan2}(k_y, k_x)$ being its polar and azimuthal angles.

The vectors $e_\lambda(\hat{k})$, $\lambda = \pm 1$ together with $e_0(\hat{k}) := \hat{k}$ build a local orthonormal basis at k. They are eigenvectors of the helicity operator $\Lambda = \frac{i\hbar k\times}{k}$:

$$\frac{i\hbar k\times}{k} e_\lambda(\hat{k}) = \lambda\hbar e_\lambda(\hat{k}), \qquad \text{for } \lambda = -1, 0, 1. \tag{7}$$

The $\lambda = \pm 1$ basis vectors are suitable for decomposition of transverse fields into parts of definite circular polarizations, since the $\lambda = 0$ fields have zero curl and do not occur in $k > 0$ Maxwell fields. To achieve the decomposition, first one performs the 3D Fourier transform of the complex electric field

$$E(r, t) = \frac{1}{\sqrt{(2\pi)^3}} \int d^3k \, \bar{E}(k) \, e^{-ikct} e^{ik\cdot r}, \tag{8}$$

with absolute value of wave vector $k = |k| = \omega/c$, and then projects the polarization vectors of helicity $\lambda = \pm 1$ onto $\bar{E}(k)$, with dimensional constants chosen for future convenience:

$$f_\lambda(k) = \sqrt{2} \sqrt{\frac{\epsilon_0}{c\hbar}} \, e_\lambda(\hat{k})^* \cdot \bar{E}(k), \tag{9}$$

so $\bar{E}(k) = \frac{1}{\sqrt{2}} \sqrt{\frac{c\hbar}{\epsilon_0}} \sum_{\lambda=\pm 1} f_\lambda(k) e_\lambda(\hat{k})$, which results in the decomposition

$$E(r, t) = \sqrt{\frac{c\hbar}{\epsilon_0}} \frac{1}{\sqrt{2}} \frac{1}{\sqrt{(2\pi)^3}} \sum_{\lambda=\pm 1} \int \frac{d^3k}{k} f_\lambda(k) k e_\lambda(\hat{k}) e^{i(k\cdot r - ckt)}, \tag{10}$$

where the coefficients $f_\lambda(k)$ obey [17] the transformation laws of a photon wave function. The independent helicity $\lambda = \pm 1$ components (left- and right-handed polarization) of the electric field are the two Riemann–Silberstein vectors $F_\lambda(r, t) = (E(r, t) + i\lambda c B(r, t))/\sqrt{2}$:

$$F_\lambda(r, t) = \frac{1}{\sqrt{(2\pi)^3}} \int d^3k \, \frac{\bar{E}(k) + i\lambda c \bar{B}(k)}{\sqrt{2}} e^{i(k\cdot r - ckt)} \tag{11}$$

$$= \frac{1}{\sqrt{2}} \frac{1}{\sqrt{(2\pi)^3}} \int d^3k \left(\bar{E}(k) + i\lambda \frac{k\times}{k} \bar{E}(k) \right) e^{i(k\cdot r - ckt)} \tag{12}$$

$$= \sqrt{\frac{c\hbar}{\epsilon_0}} \frac{1}{\sqrt{2}} \frac{1}{\sqrt{(2\pi)^3}} \int d^3k \, \frac{1}{\sqrt{2}} \Big(f_+(k) e_+(\hat{k}) + f_-(k) e_-(\hat{k}) + \lambda f_+(k) e_+(\hat{k}) - \lambda f_-(k) e_-(\hat{k}) \Big) e^{i(k\cdot r - ckt)}$$

$$= \sqrt{\frac{c\hbar}{\epsilon_0}} \frac{1}{\sqrt{(2\pi)^3}} \int \frac{d^3k}{k} f_\lambda(k) e_\lambda(\hat{k}) k e^{i(k\cdot r - ckt)}, \tag{13}$$

where we used the Maxwell equation in the wave vector space $k \times \bar{E}(k) = ck\bar{B}(k)$ in the second line of Eq. (13). Since we work with complex-valued electric and magnetic fields, the two Riemann–Silberstein vectors are independent and only together provide the complete description of the electromagnetic field: F_- for waves of the right-handed circular polarization and F_+ for the left-handed.

We define the electromagnetic plane wave as

$$\boxed{\begin{aligned} |k\,\lambda\rangle &\equiv Q_\lambda(k, r, t) \\ &= \sqrt{\frac{c\hbar}{\epsilon_0}} \frac{1}{\sqrt{2}} \frac{1}{\sqrt{(2\pi)^3}} k \, e_\lambda(\hat{k}) e^{-ikct} e^{ik\cdot r} \end{aligned}} \tag{14}$$

so the decomposition of the electromagnetic field is written as

$$E(r, t) = \sum_{\lambda=\pm 1} \int \frac{d^3k}{k} f_\lambda(k) Q_\lambda(k, r, t). \tag{15}$$

The factor k in the definition of the plane wave in Eq. (14) is important. We see that it appears because in Eq. (10) we have changed from the integration measure d^3k of the 3D Fourier transform, to the integration measure $\frac{d^3k}{k}$, which is the Lorentz invariant integration measure in the light cone [32, Eq. (2.5.15)][14, Sec. 10.4.6]. This change then introduces a factor of k in the definition of the plane wave in Eq. (14), and, as we show in Section 2.1.1, it is precisely this factor of k that makes $Q_\lambda(k, r, t)$ and $f_\lambda(k)$ transform as massless unitary irreducible representations of the Poincaré group with helicity $\lambda = \pm 1$, which are the transformation properties that the photon wave function must have, according to Wigner's classification [16]. The transformation rules are [14, Eqs. (10.4–23), (10.4–24)]:

$$T(a^\mu)|k\,\lambda\rangle = |k\,\lambda\rangle e^{-ia^\mu k_\mu} \tag{16}$$

$$R(\alpha, \beta, \gamma)|k\,\lambda\rangle = |\tilde{k}\,\lambda\rangle e^{-i\lambda\psi}, \qquad \tilde{k} = R(\alpha, \beta, \gamma)k \tag{17}$$

$$L_z(\xi)|k\,\lambda\rangle = |k'\,\lambda\rangle, \qquad k' = L_z(\xi)k \tag{18}$$

where $T(a^\mu)$ is a 4D translation in Minkowski space (we use the convention of metric signature $(-+++)$), so $a^\mu k_\mu = -a^0|k| + a \cdot k$. $R(\alpha, \beta, \gamma) = R_z(\alpha)R_y(\beta)R_z(\gamma)$ is a rotation operator with corresponding Euler angles, ψ satisfies $R(0, 0, \psi) = R(\tilde{\phi}, \tilde{\theta}, 0)^{-1} R(\alpha, \beta, \gamma) R(\phi, \theta, 0)$ ($\tilde{\phi}, \tilde{\theta}$ are spherical angles of the rotated wave vector $\tilde{k} = R(\alpha, \beta, \gamma)k$), and $L_z(\xi)$ is a Lorentz boost (Appendix B) along the z-axis with rapidity ξ. Since boosting along an arbitrary direction can be decomposed into a composition of rotations and a boost in the z-direction with Eq. (150), we will only treat explicitly the boost along the z-direction.

Plane waves in this representation transform under parity and time reversal[1] as

$$I_s|k\,\lambda\rangle = |-k\, -\lambda\rangle \tag{19}$$

$$I_t|k\,\lambda\rangle = |-k\,\lambda\rangle. \tag{20}$$

The measure $\int \frac{d^3k}{k}$ is invariant under the action of the Poincaré group, which allows one to formulate the transformation of the field by transforming the coefficients $f_\lambda(k)$ in a way similar to the basis vectors [14, Secs. 7.6 and 10.5.1]. For example, for a boost in the z-direction Eq. (18) the invariance of the measure means that $\int \frac{d^3k}{|k|} = \int \frac{d^3 L_z^{-1}(\xi)k}{|L_z^{-1}(\xi)k|}$, which, together with the linearity of the boost operator and Eq. (18) results in:

$$\begin{aligned} L_z(\xi)|f\rangle &= \sum_{\lambda=\pm 1} \int \frac{d^3k}{k} f_\lambda(k) |L_z(\xi)k\,\lambda\rangle \\ &= \sum_{\lambda=\pm 1} \int \frac{d^3 L_z^{-1}(\xi)k}{|L_z^{-1}(\xi)k|} f_\lambda(L_z^{-1}(\xi)k) |k\,\lambda\rangle \\ &= \sum_{\lambda=\pm 1} \int \frac{d^3k}{k} f_\lambda(L_z^{-1}(\xi)k) |k\,\lambda\rangle. \end{aligned} \tag{21}$$

---

[1] The time reversal is represented anti-unitarily by an operator I_t satisfying $\langle I_t\phi|I_t\psi\rangle = \langle\phi|\psi\rangle^* = \langle\psi|\phi\rangle$.

The rules for transforming the coefficients $f_\lambda(\boldsymbol{k})$ are

$$T(a^\mu)f_\lambda(\boldsymbol{k}) = f_\lambda(\boldsymbol{k})e^{-ia^\mu k_\mu}, \tag{22}$$

$$R(\alpha,\beta,\gamma)f_\lambda(\boldsymbol{k}) = f_\lambda(\tilde{\boldsymbol{k}})e^{-i\lambda\psi}, \qquad \tilde{\boldsymbol{k}} = R^{-1}(\alpha,\beta,\gamma)\boldsymbol{k} \tag{23}$$

$$L_z(\xi)f_\lambda(\boldsymbol{k}) = f_\lambda(\boldsymbol{k}'), \qquad \boldsymbol{k}' = L_z^{-1}(\xi)\boldsymbol{k} \tag{24}$$

with ψ found this time from $R(0,0,\psi) = R(\phi,\theta,0)^{-1}R(\alpha,\beta,\gamma)R(\tilde{\phi},\tilde{\theta},0)$, where $\tilde{\phi},\tilde{\theta}$ belong to the wave vector $\tilde{\boldsymbol{k}} = R^{-1}(\alpha,\beta,\gamma)\boldsymbol{k}$. The transformations under parity and time reversal are

$$I_s f_\lambda(\boldsymbol{k}) = f_{-\lambda}(-\boldsymbol{k}) \tag{25}$$

$$I_t f_\lambda(\boldsymbol{k}) = f_\lambda^*(-\boldsymbol{k}). \tag{26}$$

Transformation properties of the defined plane waves and coefficients in the decomposition Eq. (15) justify the way of writing the electric field as a ket

$$|f\rangle = \sum_{\lambda=\pm 1} \int \frac{d^3\boldsymbol{k}}{k} f_\lambda(\boldsymbol{k})|\boldsymbol{k}\lambda\rangle. \tag{27}$$

The coefficients $f_\lambda(\boldsymbol{k})$ belong to a Hilbert space with the scalar product

$$\langle f|g\rangle = \sum_{\lambda=\pm 1} \int \frac{d^3\boldsymbol{k}}{k} f_\lambda^*(\boldsymbol{k})g_\lambda(\boldsymbol{k}). \tag{28}$$

Such Hilbert space is isomorphic to the Hilbert space of solutions of Maxwell equations.

Thanks to the extra dimensional factors in Eq. (9), the $f_\lambda(\boldsymbol{k})$ have the units inverse to the wavevector, that is, meters: $[f_\lambda(\boldsymbol{k})] = $ m. The scalar product Eq. (28) is then dimensionless, which is consistent with the physical interpretation of $\langle f|f\rangle$ as the number of photons [33] contained in the field described by $|f\rangle$. The integral in [33, Eq. (1)] is a different representation of the same scalar product, as can be seen by comparing Eq. (3) and Eq. (6) in [18].

The scalar product also allows to quantify fundamental properties that are carried by the field, for example, energy, linear momentum, and angular momentum — using the expectation values $\langle f|\Gamma|f\rangle$ with Γ being the generator of the corresponding symmetry transformation: time translation for energy, spatial translation for linear momentum and rotation for angular momentum.

It is also known [18] that the scalar product in Eq. (28) is invariant under the conformal group, which is the largest group of invariance of Maxwell equations [34]. It contains the Poincaré group, and additionally special conformal transformations and dilations.

Appendix A contains a brief discussion about the representation of the vector potential and its transformation properties. In particular, the plane waves for decomposing the vector potential *do not* feature the extra factor of k.

2.1.1. Lorentz boosts $L_z(\xi)|\boldsymbol{k}\lambda\rangle$

We provide here the explicit derivation of the transformation of $\boldsymbol{Q}_\lambda(\boldsymbol{k},\boldsymbol{r},t)$ upon an *active* boost of in z-direction with rapidity ξ. The rest of the transformation properties in Eqs. (16), (17), (19), (20) are derived in Appendix C.

The transformation of general electromagnetic fields in [35, Eq. (11.149)] can be used to derive the action of the boost (see also Eq. (157)):

$$\boldsymbol{Q}_\lambda(\boldsymbol{k},\boldsymbol{r},t) = \gamma\boldsymbol{Q}_\lambda(\boldsymbol{k},\tilde{\boldsymbol{r}},\tilde{t}) + \frac{i\lambda\gamma}{c}\boldsymbol{v}\times\boldsymbol{Q}_\lambda(\boldsymbol{k},\tilde{\boldsymbol{r}},\tilde{t}) - \frac{\gamma^2\boldsymbol{v}}{(\gamma+1)c^2}\boldsymbol{v}\cdot\boldsymbol{Q}_\lambda(\boldsymbol{k},\tilde{\boldsymbol{r}},\tilde{t})$$

$$\equiv \left(\gamma\mathbb{1} + \frac{i\lambda\gamma}{c}\boldsymbol{v}\times - \frac{\gamma^2\boldsymbol{v}}{(\gamma+1)c^2}\boldsymbol{v}\cdot\right)\boldsymbol{Q}_\lambda(\boldsymbol{k},\tilde{\boldsymbol{r}},\tilde{t}), \tag{29}$$

where in Eq. (29) we factored out $\boldsymbol{Q}_\lambda$ and combined three linear operators $\mathbb{1}$, $\boldsymbol{v}\times$, and $\boldsymbol{v}\boldsymbol{v}\cdot$. Here $\boldsymbol{v} = v\boldsymbol{e}_z = c\tanh(\xi)\boldsymbol{e}_z$, $\gamma = (1 - $

$v^2/c^2)^{-1/2} = \cosh(\xi)$, $\gamma v = c\sinh(\xi)$ and space–time coordinates are inversely transformed via

$$\begin{pmatrix} c\tilde{t} \\ \tilde{\boldsymbol{r}} \end{pmatrix} = L_z^{-1}(\xi)\begin{pmatrix} ct \\ \boldsymbol{r} \end{pmatrix} = \begin{pmatrix} \cosh(\xi) & 0 & 0 & -\sinh(\xi) \\ 0 & 1 & 0 & 0 \\ 0 & 0 & 1 & 0 \\ -\sinh(\xi) & 0 & 0 & \cosh(\xi) \end{pmatrix}\begin{pmatrix} ct \\ x \\ y \\ z \end{pmatrix}. \tag{30}$$

It is important to distinguish between the passive and active versions of the Lorentz boost. In the passive version, where the reference frame is boosted instead of the field, Eqs. (29)–(30) incorporate $-\boldsymbol{v}$ in place of $\boldsymbol{v}$ (and, equivalently, $-\xi$ instead of ξ).

Since the helicity basis vectors $\boldsymbol{e}_\sigma(\hat{\boldsymbol{k}})$ can be obtained as $\boldsymbol{e}_\sigma(\hat{\boldsymbol{k}}) = R(\phi,\theta,0)\boldsymbol{e}_\sigma(\hat{\boldsymbol{z}})$, and they transform under rotations as

$$R(\alpha,\beta,\gamma)\boldsymbol{e}_\lambda(\hat{\boldsymbol{k}}) = \sum_{\sigma=\pm 1,0} D_{\sigma\lambda}^1(\alpha,\beta,\gamma)\boldsymbol{e}_\lambda(\hat{\boldsymbol{k}}) \tag{31}$$

where $D_{mn}^j(\alpha,\beta,\gamma) = e^{-im\alpha}d_{mn}^j(\beta)e^{-in\gamma}$ are Wigner matrices and $d_{mn}^j(\beta)$ are small Wigner matrices, as defined in [14], Sec. 7.3. Then:

$$\left(\gamma\mathbb{1} + \frac{i\lambda\gamma}{c}\boldsymbol{v}\times - \frac{\gamma^2\boldsymbol{v}}{(\gamma+1)c^2}\boldsymbol{v}\cdot\right)k\,\boldsymbol{e}_\lambda(\hat{\boldsymbol{k}})$$

$$= \left(\cosh(\xi)\mathbb{1} + i\lambda\sinh(\xi)\boldsymbol{e}_z\times - \frac{\sinh^2(\xi)\boldsymbol{e}_z}{\cosh(\xi)+1}\boldsymbol{e}_z\cdot\right)\sum_{\sigma=-1,0,1}D_{\sigma\lambda}^1(\phi,\theta,0)k\,\boldsymbol{e}_\sigma(\hat{\boldsymbol{z}})$$

$$= \sum_{\sigma=-1,0,1}D_{\sigma\lambda}^1(\phi,\theta,0)\left(\cosh(\xi)+\lambda\sigma\sinh(\xi)-\frac{\sinh^2(\xi)\delta_{0\sigma}}{\cosh(\xi)+1}\right)k\,\boldsymbol{e}_\sigma(\hat{\boldsymbol{z}}) \tag{32}$$

$$= \sum_{\sigma=-1,0,1}e^{-i\phi\sigma}d_{\sigma\lambda}^1(\theta)\left(\sigma\lambda\sinh(\xi)+\frac{\cosh(\xi)+\cosh^2(\xi)-\sinh^2(\xi)\delta_{0\sigma}}{\cosh(\xi)+1}\right)k\,\boldsymbol{e}_\sigma(\hat{\boldsymbol{z}})$$

$$= \sum_{\sigma=-1,0,1}e^{-i\phi\sigma}d_{\sigma\lambda}^1(\tilde{\theta})\tilde{k}\,\boldsymbol{e}_\sigma(\hat{\boldsymbol{z}}) \tag{33}$$

$$= \tilde{k}\,\boldsymbol{e}_\lambda(\hat{\tilde{\boldsymbol{k}}}). \tag{34}$$

For Eq. (32) we have used $\boldsymbol{e}_z\times\boldsymbol{e}_\sigma(\hat{\boldsymbol{z}}) = -i\sigma\boldsymbol{e}_\sigma(\hat{\boldsymbol{z}})$ and $\boldsymbol{e}_z(\boldsymbol{e}_z\cdot\boldsymbol{e}_\sigma(\hat{\boldsymbol{z}})) = \delta_{0\sigma}\boldsymbol{e}_\sigma(\hat{\boldsymbol{z}})$ for $\sigma = -1,0,1$. Eq. (33) follows from the transformation rules for the wave vector $\boldsymbol{k}$ (Appendix B):

$$\tilde{k}\,d_{0\lambda}^1(\tilde{\theta}) = \frac{\lambda\tilde{k}}{\sqrt{2}}\sin(\tilde{\theta}) = \frac{\lambda k}{\sqrt{2}}\sin(\theta) = k\,d_{0\lambda}^1(\theta) \tag{35}$$

for $\lambda = \pm 1$, $\sigma = 0$ and

$$\tilde{k}\,d_{\sigma\lambda}^1(\tilde{\theta}) = \frac{\tilde{k}}{2}\left(1 + \sigma\lambda\cos(\tilde{\theta})\right) \tag{36}$$

$$= \frac{k\left(\cosh(\xi)+\cos(\theta)\sinh(\xi)\right)}{2}\left(1 + \sigma\lambda\frac{\cos(\theta)\cosh(\xi)+\sinh(\xi)}{\cosh(\xi)+\cos(\theta)\sinh(\xi)}\right)$$

$$= \frac{k}{2}\left(\cosh(\xi)+\cos(\theta)\sinh(\xi)+\sigma\lambda(\cos(\theta)\cosh(\xi)+\sinh(\xi))\right)$$

$$= \frac{k}{2}\left(1 + \sigma\lambda\cos(\theta)\right)\left(\cosh(\xi)+\sigma\lambda\sinh(\xi)\right)$$

$$= k\,d_{\sigma\lambda}^1(\theta)\left(1 + \sigma\lambda\sinh(\xi)\right) \tag{37}$$

for $\lambda = \pm 1$, $\sigma = \pm 1$.

Together with the fact that for any Lorentz boost L

$$e^{-ik^\mu(L^{-1}x)_\mu} = e^{-i(Lk)^\mu x_\mu}, \tag{38}$$

this implies Eq. (18):

$$\boxed{\left(\gamma\mathbb{1} + \frac{i\lambda\gamma v}{c}\boldsymbol{e}_z\times - \frac{\gamma^2 v^2\boldsymbol{e}_z}{(\gamma+1)c^2}\boldsymbol{e}_z\cdot\right)\boldsymbol{Q}_\lambda(\boldsymbol{k},\tilde{\boldsymbol{r}},\tilde{t}) = \boldsymbol{Q}_\lambda(\tilde{\boldsymbol{k}},\boldsymbol{r},t).} \tag{39}$$

We emphasize that without the k-factor in the definition Eq. (14), the plane wave would not transform according to the unitary representation Eq. (18).

2.2. Angular momentum basis for regular fields $|kjm\lambda\rangle$

The multipolar fields, also known as vector spherical harmonics or angular momentum fields, play a crucial role in the T-matrix formalism: they constitute the basis with respect to which the fields are expanded.

The angular momentum basis can be defined with respect to the plane wave basis as [14, Sec. 8.4.1]:

$$|kjm\lambda\rangle = \sqrt{\frac{2j+1}{4\pi}} \int_0^{2\pi} d\phi \int_{-1}^{1} d(\cos\theta)\, D_{m\lambda}^j(\phi,\theta,0)^* |k\lambda\rangle \qquad (40)$$

$$|k\lambda\rangle = \sum_{j=1}^{\infty} \sum_{m=-j}^{j} \sqrt{\frac{2j+1}{4\pi}} D_{m\lambda}^j(\phi,\theta,0) |kjm\lambda\rangle \qquad (41)$$

with the corresponding connection between coefficients in the angular momentum and the plane wave basis

$$f_{jm\lambda}(k) = \sqrt{\frac{2j+1}{4\pi}} \int_0^{2\pi} d\phi \int_{-1}^{1} d(\cos\theta)\, D_{m\lambda}^j(\phi,\theta,0)\, f_\lambda(\mathbf{k}) \qquad (42)$$

$$f_\lambda(\mathbf{k}) = \sum_{j=1}^{\infty} \sum_{m=-j}^{j} \sqrt{\frac{2j+1}{4\pi}} D_{m\lambda}^j(\phi,\theta,0)^* f_{jm\lambda}(k). \qquad (43)$$

The indices in $|kjm\lambda\rangle$ correspond to eigenvalues of Hermitian operators of energy H, total angular momentum $J^2 = J_x^2 + J_y^2 + J_z^2$, angular momentum along z-axis J_z, and helicity Λ:

$$H|kjm\lambda\rangle = \hbar c k |kjm\lambda\rangle$$
$$J^2|kjm\lambda\rangle = \hbar^2 j(j+1)|kjm\lambda\rangle, \quad j = 1, 2, \dots$$
$$J_z|kjm\lambda\rangle = \hbar m|kjm\lambda\rangle, \qquad m = -j, -j+1, \dots, j$$
$$\Lambda|kjm\lambda\rangle = \hbar\lambda|kjm\lambda\rangle, \qquad \lambda = \pm 1.$$

In particular, $j = 1$ corresponds to the dipolar fields, $j = 2$ corresponds to the quadrupolar fields, and so on. We remark for completeness that the plane waves are eigenstates of helicity $\Lambda|k\lambda\rangle = \hbar\lambda|k\lambda\rangle$, and of the three translation operators, and hence of their Hermitian generators, the linear momentum operators $P_{x,y,z}|k\lambda\rangle = \hbar k_{x,y,z}|k\lambda\rangle$.

A state can be represented in the angular momentum basis by using Eqs. (40)–(43) in Eq. (27), which results in

$$|f\rangle = \int_0^{\infty} dk\, k \sum_{\lambda=\pm 1} \sum_{j=1}^{\infty} \sum_{m=-j}^{j} f_{jm\lambda}(k)|kjm\lambda\rangle \qquad (44)$$

and the scalar product in Eq. (28) can correspondingly be written in the angular momentum basis as

$$\langle g|f\rangle = \sum_{\lambda=\pm 1} \int_0^{\infty} dk\, k \sum_{j=1}^{\infty} \sum_{m=-j}^{j} g_{jm\lambda}^*(k) f_{jm\lambda}(k). \qquad (45)$$

We note that coefficients $f_{jm\lambda}(k)$ have the units of meters just as $f_\lambda(\mathbf{k})$.

This allows one to obtain explicit $(\mathbf{r}, t)$-dependent expressions of the angular momentum basis $|kjm\lambda\rangle$ for the regular electromagnetic field as follows:

$$\mathbf{R}_{jm\lambda}(k,\mathbf{r},t) = \sqrt{\frac{2j+1}{4\pi}} \int_0^{2\pi} d\phi \int_{-1}^{1} d(\cos\theta)\, D_{m\lambda}^j(\phi,\theta,0)^* \mathbf{Q}_\lambda(\mathbf{k},\mathbf{r},t)$$
$$= \sqrt{\frac{c\hbar}{\epsilon_0}} \frac{k\, e^{-ikct}}{\sqrt{2}\sqrt{(2\pi)^3}} \sqrt{\frac{2j+1}{4\pi}} \int_0^{2\pi} d\phi \int_{-1}^{1} d(\cos\theta)\, D_{m\lambda}^j(\phi,\theta,0)^* \mathbf{e}_\lambda(\hat{\mathbf{k}}) e^{i\mathbf{k}\cdot\mathbf{r}}, \qquad (46)$$

where the integration proceeds over the polar and azimuthal angles (θ, ϕ) of the wave vector. The integration results in

$$\mathbf{R}_{jm\lambda}(k,\mathbf{r},t) = \sqrt{\frac{c\hbar}{\epsilon_0}} \frac{k\, e^{-ikct}}{\sqrt{\pi}\sqrt{2j+1}} \sum_{L=j-1}^{j+1} \sqrt{2L+1}\, i^L j_L(kr)\, C_{L0,1\lambda}^{j\lambda} \mathbf{Y}_{jm}^L(\hat{\mathbf{r}}) \qquad (47)$$

$$\equiv |kjm\lambda\rangle$$

with Clebsch–Gordan coefficients $C_{j_1 m_1 j_2 m_2}^{j_3 m_3}$ and vector spherical harmonics [31, Sec. 7.3.1]

$$\mathbf{Y}_{jm}^L(\hat{\mathbf{r}}) = \sqrt{\frac{2L+1}{4\pi}} \sum_{\sigma=\pm 1,0} \mathbf{e}_\sigma(\hat{\mathbf{z}}) D_{m-\sigma,0}^L(\phi,\theta,0)^* C_{Lm-\sigma,1\sigma}^{jm}. \qquad (48)$$

The decomposition of the regular electromagnetic field $\mathbf{E}(\mathbf{r},t)$ then reads, as suggested by Eq. (44)

$$\mathbf{E}(\mathbf{r},t) = \int_0^{\infty} dk\, k \sum_{\lambda=\pm 1} \sum_{j=1}^{\infty} \sum_{m=-j}^{j} f_{jm\lambda}(k)\mathbf{R}_{jm\lambda}(k,\mathbf{r},t). \qquad (49)$$

The connection between $\mathbf{R}_{jm\lambda}(k,\mathbf{r},t)$ and the usual regular electric and magnetic multipoles

$$\mathbf{N}_{jm}(kr,\hat{\mathbf{r}}) = ij_{j-1}(kr)\sqrt{\frac{j+1}{2j+1}}\mathbf{Y}_{jm}^{j-1}(\hat{\mathbf{r}}) - ij_{j+1}(kr)\sqrt{\frac{j}{2j+1}}\mathbf{Y}_{jm}^{j+1}(\hat{\mathbf{r}}) \qquad (50)$$

$$\mathbf{M}_{jm}(kr,\hat{\mathbf{r}}) = j_j(kr)\mathbf{Y}_{jm}^j(\hat{\mathbf{r}}) \qquad (51)$$

can be found using the expression for Clebsch–Gordan coefficients

$$C_{L0,1\lambda}^{j\lambda} = \begin{cases} \sqrt{\dfrac{j}{2(2j+3)}}, & \text{if } L = j+1 \\[2mm] -\dfrac{\lambda}{\sqrt{2}}, & \text{if } L = j \\[2mm] \sqrt{\dfrac{(j+1)}{2(2j-1)}}, & \text{if } L = j-1 \end{cases} \qquad (52)$$

for $\lambda = \pm 1$. The relation is then

$$\boxed{\begin{aligned} |kjm\lambda\rangle &\equiv \mathbf{R}_{jm\lambda}(k,\mathbf{r},t) \\ &= -\sqrt{\frac{c\hbar}{\epsilon_0}}\frac{1}{\sqrt{2\pi}}k\, i^j\left(e^{-ikct}\mathbf{N}_{jm}(kr,\hat{\mathbf{r}}) + \lambda e^{-ikct}\mathbf{M}_{jm}(kr,\hat{\mathbf{r}})\right) \end{aligned}} \qquad (53)$$

with corresponding inverse relations

$$e^{-ikct}\mathbf{N}_{jm}(kr,\hat{\mathbf{r}}) = -\sqrt{\frac{\epsilon_0}{c\hbar}}\frac{1}{2}\left(\mathbf{R}_{jm+}(k,\mathbf{r},t) + \mathbf{R}_{jm-}(k,\mathbf{r},t)\right)\frac{(-i)^j\sqrt{2\pi}}{k} \qquad (54)$$

$$e^{-ikct}\mathbf{M}_{jm}(kr,\hat{\mathbf{r}}) = -\sqrt{\frac{\epsilon_0}{c\hbar}}\frac{1}{2}\left(\mathbf{R}_{jm+}(k,\mathbf{r},t) - \mathbf{R}_{jm-}(k,\mathbf{r},t)\right)\frac{(-i)^j\sqrt{2\pi}}{k}. \qquad (55)$$

We note that the factor of k in the plane wave definition of Eq. (14) leads to the extra factor of k in the angular momentum basis in Eq. (53) compared to the usual multipolar basis $\mathbf{M}$ and $\mathbf{N}$. Such difference ensures that $\mathbf{R}_{jm\lambda}(k,\mathbf{r},t)$ have the same transformation laws as $|kjm\lambda\rangle$ under the action of the Poincaré group (see Sec. 2.2.2). The $|kjm\lambda\rangle$ transform unitarily in particular under Lorentz boosts because the $|kjm\lambda\rangle$ are unitarily connected to $|k\lambda\rangle$ by Eq. (40), and we have already shown that the $|k\lambda\rangle$ transform unitarily under Lorentz boosts.

Computing the T-matrix of an object moving with constant speed from the T-matrix of the object at rest requires the Lorentz boost of the T-matrix at rest. The T-matrix connects regular incident fields with irregular outgoing fields, and one cannot a priori assume that the two kinds of fields transform identically under boosts. Yet, that is indeed the case, as we proof in Section 2.3.1. Therefore, knowledge of the boost matrix in the regular angular momentum basis, which we derive in Section 2.2.1, is sufficient for boosting T-matrices. The transformation properties of the $|kjm\lambda\rangle$ under other transformations can be found in Section 2.2.2.

2.2.1. Matrix element of Lorentz boosts $\langle k_1 j_1 m_1 \lambda_1 | L_z(\xi) | k_2 j_2 m_2 \lambda_2 \rangle$

Here we derive the matrix element of the Lorentz boost along the z-direction in the angular momentum basis. The core idea of the derivation consists in switching to the plane wave basis via Eqs. (40)–(41) and utilizing the known transformation property of the plane waves Eq. (18). Subsequently, we switch back to the angular momentum basis.

We will refer to the plane wave basis states $|k\lambda\rangle$ as $|k\theta\phi\lambda\rangle$ with θ and ϕ denoting the spherical angles of the wavevector for convenience.

$$L_z(\xi)|k_2 j_2 m_2 \lambda_2\rangle =$$
$$= L_z(\xi)\sqrt{\frac{2j_2+1}{4\pi}} \int_0^{2\pi} d\phi_2 \int_{-1}^{1} d(\cos\theta_2)\, D_{m_2\lambda_2}^{j_2}(\phi_2,\theta_2,0)^* |k_2\theta_2\phi_2\lambda_2\rangle$$
$$= \sqrt{\frac{2j_2+1}{4\pi}} \int_0^{2\pi} d\phi_2 \int_{-1}^{1} d(\cos\theta_2)\, D_{m_2\lambda_2}^{j_2}(\phi_2,\theta_2,0)^* |k_1\theta_1\phi_2\lambda_2\rangle \qquad (56)$$

with boosted plane wave $|k_1\theta_1\phi_2\lambda_2\rangle$ according to Eq. (18). Its azimuthal angle ϕ_2 and helicity λ_2 are unchanged, the wavenumber and the polar angles are transformed according to (Appendix B):

$$\cos(\theta_1) = \frac{\cos(\theta_2) + \tanh(\xi)}{1 + \cos(\theta_2)\tanh(\xi)} \tag{57}$$

$$k_1 = k_2(\cosh(\xi) + \cos(\theta_2)\sinh(\xi)). \tag{58}$$

Writing the transformed plane wave in the angular momentum basis gives

$$L_z(\xi)|k_2 j_2 m_2 \lambda_2\rangle = \sqrt{\frac{2j_2+1}{4\pi}} \int_0^{2\pi} d\phi_2 \int_{-1}^1 d(\cos\theta_2) D_{m_2\lambda_2}^{j_2}(\phi_2,\theta_2,0)^*$$

$$\times \sum_{j_1=1}^\infty \sum_{m_1=-j_1}^{j_1} \sqrt{\frac{2j_1+1}{4\pi}} D_{m_1\lambda_2}^{j_1}(\phi_2,\theta_1,0)|k_1 j_1 m_1 \lambda_2\rangle \tag{59}$$

$$= \frac{1}{2} \int_{-1}^1 d(\cos\theta_2) \sum_{j_1=1}^\infty \sqrt{2j_1+1}\sqrt{2j_2+1}\, d_{m_2\lambda_2}^{j_1}$$

$$\times (\theta_1) d_{m_2\lambda_2}^{j_2}(\theta_2)|k_1 j_1 m_2 \lambda_2\rangle, \tag{60}$$

where the last step involved integration over ϕ_2. It is possible to write this expression in terms of the integral over the wavenumber by substitution defined via Eq. (58):

$$L_z(\xi)|k_2 j_2 m_2 \lambda_2\rangle =$$

$$= \frac{1}{2} \int_{k_2 e^{-\xi}}^{k_2 e^{\xi}} \frac{dk_1}{k_2 \sinh(\xi)} \sum_{j_1=1}^\infty \sqrt{2j_1+1}\sqrt{2j_2+1}\, d_{m_2\lambda_2}^{j_1}(\theta_1) d_{m_2\lambda_2}^{j_2}(\theta_2)|k_1 j_1 m_2 \lambda_2\rangle \tag{61}$$

$$= \frac{1}{2} \int_{k_2 e^{-|\xi|}}^{k_2 e^{|\xi|}} \frac{dk_1}{k_2 \sinh(|\xi|)} \sum_{j_1=1}^\infty \sqrt{2j_1+1}\sqrt{2j_2+1}\, d_{m_2\lambda_2}^{j_1}(\theta_1) d_{m_2\lambda_2}^{j_2}(\theta_2)|k_1 j_1 m_2 \lambda_2\rangle. \tag{62}$$

The derived equations hold for both positive and negative ξ that correspond to movement in positive and negative z-direction. The Eq. (61) is the closed form expression equivalent to Eq. (5.15) in [36].

The matrix element of the Lorentz boost is defined to satisfy

$$L_z(\xi)|k_2 j_2 m_2 \lambda_2\rangle =$$

$$= \int_0^\infty dk_1\, k_1 \sum_{\lambda_1=\pm 1} \sum_{j_1=1}^\infty \sum_{m_1=-j_1}^{j_1} |k_1 j_1 m_1 \lambda_1\rangle\langle k_1 j_1 m_1 \lambda_1|L_z(\xi)|k_2 j_2 m_2 \lambda_2\rangle. \tag{63}$$

Bringing Eq. (62) in this form leads to

$$\boxed{\begin{aligned}&\langle k_1 j_1 m_1 \lambda_1|L_z(\xi)|k_2 j_2 m_2 \lambda_2\rangle = \\ &= \delta_{m_1 m_2}\delta_{\lambda_1\lambda_2}\Theta\big(|\xi| - |\ln(k_1/k_2)|\big)\frac{\sqrt{2j_1+1}\sqrt{2j_2+1}}{2k_1 k_2 \sinh(|\xi|)} d_{m_1\lambda_1}^{j_1}(\theta_1) d_{m_2\lambda_2}^{j_2}(\theta_2)\end{aligned}}$$

with

$$\cos\theta_1 = \frac{k_1 \cosh(\xi) - k_2}{k_1 \sinh(\xi)} \tag{64}$$

$$\cos\theta_2 = \frac{k_1 - k_2 \cosh(\xi)}{k_2 \sinh(\xi)}. \tag{65}$$

The Heaviside function

$$\Theta(x) = \begin{cases} 1, & \text{if } x \geq 0 \\ 0, & \text{if } x < 0 \end{cases} \tag{66}$$

accounts for the correct spectrum of boosted wave numbers $e^{-|\xi|} \leq k_1/k_2 \leq e^{|\xi|}$:

$$\int_0^\infty dk_1\, \Theta\big(|\xi| - |\ln(k_1/k_2)|\big) = \int_{k_2 e^{-|\xi|}}^{k_2 e^{|\xi|}} dk_1. \tag{67}$$

We note that setting rapidity $\xi = 0$ in Eqs. (57), (58), (60) leads to

$$L_z(0)|k_2 j_2 m_2 \lambda_2\rangle = \frac{1}{2}\sqrt{2j_2+1} \sum_{j_1=1}^\infty \sqrt{2j_1+1}$$

$$\times \int_{-1}^1 d(\cos\theta_2) d_{m_2\lambda_2}^{j_2}(\theta_2) d_{m_2\lambda_2}^{j_1}(\theta_2)|k_2 j_1 m_2 \lambda_2\rangle$$

$$= \sum_{j_1=1}^\infty \delta_{j_1 j_2}|k_2 j_1 m_2 \lambda_2\rangle = |k_2 j_2 m_2 \lambda_2\rangle, \tag{68}$$

where we used the well-known orthogonality of small Wigner matrices:

$$\frac{1}{2}\sqrt{2j+1}\sqrt{2j'+1} \int_{-1}^1 d(\cos\theta) d_{m\lambda}^j(\theta) d_{m\lambda}^{j'}(\theta) = \delta_{jj'}. \tag{69}$$

This presents the expected result that the zero velocity Lorentz boost acts as the identity operator.

We emphasize that the derived law for transformation of $|kjm\lambda\rangle$ describes the transformation properties of basis vector fields $\boldsymbol{R}_{jm\lambda}(k,\boldsymbol{r},t)$ for all space–time points $(\boldsymbol{r},t)$.

2.2.2. List of transformations for $|kjm\lambda\rangle$

The complete list of transformation laws of the angular momentum basis states under the isometries of the Minkowski space–time reads:

$$T_t(\tau)|kjm\lambda\rangle = |kjm\lambda\rangle e^{ikc\tau} \tag{70}$$

$$T_z(a)|kjm\lambda\rangle = \sum_{j'=1}^\infty \sqrt{\frac{2j'+1}{2j+1}} \sum_{l=|j-j'|}^{j+j'} (2l+1)(-i)^l j_l(ak) C_{j'm,l0}^{jm} C_{j'\lambda,l0}^{j\lambda}|kj'm\lambda\rangle, \tag{71}$$

$$R(\alpha,\beta,\gamma)|kjm\lambda\rangle = \sum_{m'=-j}^j D_{m'm}^j(\alpha,\beta,\gamma)|kjm'\lambda\rangle \tag{72}$$

$$L_z(\xi)|kjm\lambda\rangle = \frac{1}{2}\sqrt{2j+1} \sum_{j'=1}^\infty \sqrt{2j'+1} \int_{-1}^1 d(\cos\theta) d_{m\lambda}^j(\theta) d_{m\lambda}^{j'}(\theta')|k'j'm\lambda\rangle \tag{73}$$

where θ' and k' are related to θ and k via Eqs. (57)–(58). $T_t(\tau)$ is the time translation by τ, $T_z(a)$ is the translation in the positive z-direction by a, and the translation in the general direction $\hat{n}(\alpha,\beta)$ can be described by $T_{\hat{n}}(\xi) = R(\alpha,\beta,0)T_z(a)R^{-1}(\alpha,\beta,0)$ in the similar way as general Lorentz boosts.

The actions of parity and time reversal are given by (See Appendix D)

$$I_s|kjm\lambda\rangle = |kjm-\lambda\rangle(-1)^j \tag{74}$$

$$I_t|kjm\lambda\rangle = -|kj-m\lambda\rangle(-1)^{j+m}. \tag{75}$$

The corresponding rules for transformations of coefficients are

$$T_t(\tau)f_{jm\lambda}(k) = f_{jm\lambda}(k)e^{ikc\tau} \tag{76}$$

$$T_z(a)f_{jm\lambda}(k) = \sum_{j'=1}^\infty \sqrt{\frac{2j+1}{2j'+1}} \sum_{l=|j-j'|}^{j+j'} (2l+1)(-i)^l j_l(ak) C_{jm,l0}^{j'm} C_{j\lambda,l0}^{j'\lambda} f_{j'm\lambda}(k), \tag{77}$$

$$R(\alpha,\beta,\gamma)f_{jm\lambda}(k) = \sum_{m'=-j}^j D_{mm'}^j(\alpha,\beta,\gamma) f_{jm'\lambda}(k), \tag{78}$$

$$L_z(\xi)f_{jm\lambda}(k) = \frac{1}{2}\sqrt{2j+1} \sum_{j'=1}^\infty \sqrt{2j'+1} \int_{-1}^1 d(\cos\theta) d_{m\lambda}^j(\theta) d_{m\lambda}^{j'}(\theta')f_{j'm\lambda}(k') \tag{79}$$

with θ' and k' given by

$$\cos(\theta') = \frac{\cos(\theta) - \tanh(\xi)}{1 - \cos(\theta)\tanh(\xi)}, \tag{80}$$

$$k' = k(\cosh(\xi) - \cos(\theta)\sinh(\xi)). \tag{81}$$

The actions of parity and time reversal are

$$I_s f_{jm\lambda}(k) = f_{jm-\lambda}(k)(-1)^j \tag{82}$$

$$I_t f_{jm\lambda}(k) = -f_{j-m\lambda}^*(k)(-1)^{j+m}. \tag{83}$$

2.3. Angular momentum basis for irregular fields $|kjm\lambda\rangle^{\text{in/out}}$

Besides the regular angular momentum basis vectors, which are used to expand the incident field, the T-matrix formalism also uses

the irregular outgoing angular momentum basis vectors to expand the scattered field. In the S-matrix formalism only irregular fields are used, to expand the incoming and outgoing fields. Physically, the energy flux of outgoing fields is outwards from the origin, while the flux is inwards towards the origin for the incoming fields. The regular fields have zero net flux. Mathematically, the difference between irregular and regular fields consists in the function responsible for the radial dependence: spherical Hankel functions of certain type for irregular fields instead of the spherical Bessel functions in Eq. (47) for regular fields. The Hankel functions have a singularity at $|r| = 0$. We define the incoming/outgoing states as:

$$
\begin{aligned}
|kjm\lambda\rangle^{\text{in/out}} &\equiv S_{jm\lambda}^{\text{in/out}}(k, \boldsymbol{r}, t) = \\
&\frac{1}{2}\sqrt{\frac{c\hbar}{\epsilon_0}}\frac{k\,e^{-ikct}}{\sqrt{\pi}\sqrt{2j+1}}\sum_{L=j-1}^{j+1}\sqrt{2L+1}\,i^L h_L^{\text{in/out}}(kr)\,C_{L0,1\lambda}^{j\lambda}\,Y_{jm}^L(\hat{\boldsymbol{r}})
\end{aligned}
$$

(84)

with spherical Hankel functions $h_L^{\text{in/out}} = j_L \mp i n_L$, n_L being the spherical Neumann functions.

The usual incoming/outgoing electric and magnetic multipoles are defined by substituting spherical Hankel functions of the second/first kind instead of the spherical Bessel functions in the regular multipoles in Eqs. (50)–(51):

$$
N_{jm}^{\text{in/out}}(kr, \hat{\boldsymbol{r}}) = i h_{j-1}^{\text{in/out}}(kr)\sqrt{\frac{j+1}{2j+1}}Y_{jm}^{j-1}(\hat{\boldsymbol{r}}) - i h_{j+1}^{\text{in/out}}(kr)\sqrt{\frac{j}{2j+1}}Y_{jm}^{j+1}(\hat{\boldsymbol{r}})
$$

(85)

$$
M_{jm}^{\text{in/out}}(kr, \hat{\boldsymbol{r}}) = h_j^{\text{in/out}}(kr)Y_{jm}^j(\hat{\boldsymbol{r}}).
$$

(86)

The $|kjm\lambda\rangle^{\text{in/out}}$ can then also be written as:

$$
S_{jm\lambda}^{\text{in/out}}(k, \boldsymbol{r}, t) = -\frac{1}{2}\sqrt{\frac{c\hbar}{\epsilon_0}}\frac{1}{\sqrt{2\pi}}k\,i^j\left(e^{-ikct}\,N_{jm}^{\text{in/out}}(kr, \hat{\boldsymbol{r}}) + \lambda\,e^{-ikct}\,M_{jm}^{\text{in/out}}(kr, \hat{\boldsymbol{r}})\right).
$$

(87)

We highlight that an extra factor of $1/2$ in this definition leads to

$$
S_{jm\lambda}^{\text{in}} + S_{jm\lambda}^{\text{out}} = R_{jm\lambda},
$$

(88)

the motivation and significance of which will be explained in Section 2.3.2.

The fact that irregular basis states $S_{jm\lambda}^{\text{in/out}}$ transform as the regular fields $R_{jm\lambda}$ under spatial translations and rotations is known [15]. It is evident from the definition in Eq. (84) that irregular basis states also transform as the regular basis states under time translation. Their behavior under parity and time reversal are discussed in Appendix D. In the next subsection we show that the irregular $|kjm\lambda\rangle^{\text{in/out}}$ transform under Lorentz boosts as the regular $|kjm\lambda\rangle$, completing the picture of their transformations under all isometries of the Minkowski space–time. This result is necessary for properly connecting the T-matrix and S-matrix formalisms to the Poincaré group.

2.3.1. Irregular fields transform under boosts as regular fields

In this section we discuss the transformation law for irregular basis vectors $S_{jm\lambda}(k, \boldsymbol{r}, t)$ corresponding to either incoming or outgoing basis states in Eq. (84). We show that they transform in the same way as the regular basis vectors $R_{jm\lambda}(k, \boldsymbol{r}, t)$, according to Eq. (60):

$$
S_{jm\lambda}^{\text{in/out}}(k, \boldsymbol{r}, t) \mapsto \frac{1}{2}\sqrt{2j+1}\sum_{j'=1}^{\infty}\sqrt{2j'+1}
$$

$$
\times \int_{-1}^{1}d(\cos\theta)\,d_{m\lambda}^j(\theta)\,d_{m\lambda}^{j'}(\theta')\,S_{j'm\lambda}^{\text{in/out}}(k', \boldsymbol{r}, t)
$$

(89)

Since the general formula for boosting electromagnetic field is independent of its type, Eq. (157) implies that

$$
S_{jm\lambda}^{\text{in/out}}(k, \boldsymbol{r}, t) \to \left(\cosh(\xi)\mathbb{1} + i\lambda\sinh(\xi)e_z \times - \frac{\sinh^2(\xi)e_z}{\cosh(\xi)+1}e_z\cdot\right)S_{jm\lambda}^{\text{in/out}}(k, \tilde{\boldsymbol{r}}, \tilde{t})
$$

(90)

and since Lorentz boosts in the z-direction constitute a one-parameter Lie group, it is enough to prove the following equality of derivatives w.r.t. ξ at zero:

$$
\partial_\xi \frac{1}{2}\sqrt{2j+1}\sum_{j'=1}^{\infty}\sqrt{2j'+1}\int_{-1}^{1}d(\cos\theta)\,d_{m\lambda}^j(\theta)\,d_{m\lambda}^{j'}(\theta')\,S_{j'm\lambda}^{\text{in/out}}(k', \boldsymbol{r}, t)\Big|_{\xi=0}
$$

$$
= \partial_\xi\left(\cosh(\xi)\mathbb{1} + i\lambda\sinh(\xi)e_z \times - \frac{\sinh^2(\xi)e_z}{\cosh(\xi)+1}e_z\cdot\right)S_{jm\lambda}^{\text{in/out}}(k, \tilde{\boldsymbol{r}}, \tilde{t})\Big|_{\xi=0}.
$$

(91)

The proof is also simplified by the fact that regular fields already satisfy this condition and the only difference consists in the functions responsible for the radial dependence (spherical Hankel functions instead of spherical Bessel functions). Lengthy but straightforward calculations allow one to re-write Eq. (91) (and the analogous expression for regular fields as well) by separating the radial and angular dependencies of both sides as

$$
rh_0^{\text{in/out}}(r)A(\hat{\boldsymbol{r}}, t) + rh_1^{\text{in/out}}(r)B(\hat{\boldsymbol{r}}, t) + \sum_{l=0}^{N}h_l^{\text{in/out}}(r)C_l(\hat{\boldsymbol{r}}, t)
$$

$$
= rh_0^{\text{in/out}}(r)A'(\hat{\boldsymbol{r}}, t) + rh_1^{\text{in/out}}(r)B'(\hat{\boldsymbol{r}}, t) + \sum_{l=0}^{N}h_l^{\text{in/out}}(r)C_l'(\hat{\boldsymbol{r}}, t),
$$

(92)

where the decomposition with primed coefficient functions corresponds to the right hand side of Eq. (91) and the unprimed one to the left hand side. N is finite, and for readability and without loss of generality we set $k = 1$.

We use the fact that the statement in question already holds for regular fields, which means that exactly the same coefficients solve the equation for spherical Bessel functions:

$$
rj_0(r)A(\hat{\boldsymbol{r}}, t) + rj_1(r)B(\hat{\boldsymbol{r}}, t) + \sum_{l=0}^{N}j_l(r)C_l(\hat{\boldsymbol{r}}, t)
$$

$$
= rj_0(r)A'(\hat{\boldsymbol{r}}, t) + rj_1(r)B'(\hat{\boldsymbol{r}}, t) + \sum_{l=0}^{N}j_l(r)C_l'(\hat{\boldsymbol{r}}, t).
$$

(93)

Writing

$$
\sin(r)A(\hat{\boldsymbol{r}}, t) + \left(\frac{\sin(r)}{r} - \cos(r)\right)B(\hat{\boldsymbol{r}}, t) + \sum_{l=0}^{N}j_l(r)C_l(\hat{\boldsymbol{r}}, t)
$$

$$
= \sin(r)A'(\hat{\boldsymbol{r}}, t) + \left(\frac{\sin(r)}{r} - \cos(r)\right)B'(\hat{\boldsymbol{r}}, t) + \sum_{l=0}^{N}j_l(r)C_l'(\hat{\boldsymbol{r}}, t)
$$

(94)

one notes that in the limit $r \to \infty$ the spherical Bessel functions and $\frac{\sin(r)}{r}$ vanish, hence the coefficients at $\sin$ and $\cos$ functions must be equal: $A(\hat{\boldsymbol{r}}, t) = A'(\hat{\boldsymbol{r}}, t)$ and $B(\hat{\boldsymbol{r}}, t) = B'(\hat{\boldsymbol{r}}, t)$. Then, from

$$
\sum_{l=0}^{N}j_l(r)C_l(\hat{\boldsymbol{r}}, t) = \sum_{l=0}^{N}j_l(r)C_l'(\hat{\boldsymbol{r}}, t)
$$

(95)

and the orthogonality of spherical Bessel functions follows the equality $C_l(\hat{\boldsymbol{r}}, t) = C_l'(\hat{\boldsymbol{r}}, t)$ for all k. This proves the statement for the Hankel functions Eq. (92), as well as for any functions that satisfy the same differential equation as spherical Bessel functions.

2.3.2. Relation between incoming, outgoing, and regular fields

Consider a regular electromagnetic pulse with a Gaussian profile of width Δ in $k = \omega/c$

$$
E_{\text{p}}(\boldsymbol{r}, t) = A\int_0^{\infty}dk\,k\,e^{-\frac{(k-k_0)^2}{2\Delta^2}}\,R_{jm\lambda}(k, \boldsymbol{r}, t),
$$

(96)

normalized with some constant A, and that is constructed as a spectral superposition of regular basis vector fields $\boldsymbol{R}_{jm\lambda}(k, \boldsymbol{r}, t)$ with some fixed j, m and λ. It can be decomposed into incoming and outgoing parts using the connection between spherical Bessel and Hankel functions $j = (h^{\text{in}} + h^{\text{out}})/2$ as

$$\boldsymbol{E}_{\text{p}}(\boldsymbol{r}, t) = \boldsymbol{E}_{\text{p}}^{\text{in}}(\boldsymbol{r}, t) + \boldsymbol{E}_{\text{p}}^{\text{out}}(\boldsymbol{r}, t) \tag{97}$$

with

$$\boldsymbol{E}_{\text{p}}^{\text{in}}(\boldsymbol{r}, t) = A \int_0^\infty dk \, k \, e^{-\frac{(k-k_0)^2}{2\Delta^2}} \boldsymbol{S}_{jm\lambda}^{\text{in}}(k, \boldsymbol{r}, t) \tag{98}$$

$$\boldsymbol{E}_{\text{p}}^{\text{out}}(\boldsymbol{r}, t) = A \int_0^\infty dk \, k \, e^{-\frac{(k-k_0)^2}{2\Delta^2}} \boldsymbol{S}_{jm\lambda}^{\text{out}}(k, \boldsymbol{r}, t) \tag{99}$$

for $|\boldsymbol{r}| > 0$.

The regular pulse $\boldsymbol{E}_p(\boldsymbol{r}, t)$ has finite length, so it is possible to define a time period before the pulse first reaches the origin at $\boldsymbol{r} = \boldsymbol{0}$, and a time period after the pulse has completely crossed the origin. During the first period the pulse completely consists of the incoming part

$$\boldsymbol{E}_{\text{p}}(\boldsymbol{r}, t) = \boldsymbol{E}_{\text{p}}^{\text{in}}(\boldsymbol{r}, t) \tag{100}$$

while $\boldsymbol{E}_{\text{p}}^{\text{out}}(\boldsymbol{r}, t) = 0$, and during the second period it solely consists of the outgoing part

$$\boldsymbol{E}_{\text{p}}(\boldsymbol{r}, t) = \boldsymbol{E}_{\text{p}}^{\text{out}}(\boldsymbol{r}, t) \tag{101}$$

while $\boldsymbol{E}_{\text{p}}^{\text{in}}(\boldsymbol{r}, t) = 0$.

A representative example is shown on Fig. 1. We plot numerically computed values of concrete Gaussian pulses Eqs. (96), (98), (99) with center wavelength $\frac{2\pi}{k_0} = 400$ nm, Gaussian width $\Delta^{-1} = 300$ nm, total angular momentum $j = 1$, angular momentum around z-axis $m = 1$ and helicity $\lambda = 1$. The integrals are truncated to the region $3 \, \mu m^{-1} \leq k \leq 28 \, \mu m^{-1}$, which includes the Gaussian profile of the wave function apart from a practically insignificant portion. The values of the integrals are computed via the Riemann sum with number of points $N_k = 150$. The radius of the displayed space region is 6.4 μm. The points near the origin of coordinates are disregarded in the plots of irregular fields because of the divergence of the Hankel functions.

The time stamps are selected to be within the two periods defined above, when irregular pulses are either equal to the regular pulse or identically zero. In these periods, the substitution of irregular basis fields by regular basis fields would not change the value of the total field of the pulse, which can be useful for practical applications because the spherical Bessel functions in regular fields are numerically better behaved than the spherical Hankel functions [37, App. B]. The notable split illustrated in Fig. 1 does not happen for monochromatic fields, e.g. when beams of infinite duration are involved, because at each point of time and space the regular field contains contributions from both incoming and outgoing components.

In general, such connection is present in regions of space–time when the regular field is known to contain only an incoming or only an outgoing part.

Now, if we consider coefficients $f_{jm\lambda}(k)$ that have finite norm $\langle f|f \rangle$, then, when combined with regular basis fields $\boldsymbol{R}$, they describe a regular freely propagating physical field. When the same coefficients are combined with outgoing basis fields $\boldsymbol{S}^{\text{out}}$, they describe an emitted electromagnetic field that is zero before the start of the emission and that is identically equal to the corresponding regular field at times after the end of the emission. On the other hand, when $f_{jm\lambda}(k)$ are combined with incoming basis fields $\boldsymbol{S}^{\text{in}}$, the linear combination will result in an electromagnetic field that will be absorbed during some time, such that after this period the field will be zero and before the start of the absorption the field will be identically equal to the regular field combined with the same coefficients. This allows one to connect irregular fields to the Hilbert space formalism and to use the same scalar product Eqs. (28), (45) to, in particular, compute quantities of emitted or absorbed fields, such as energy and momentum. While using

the ket notation, we will distinguish incoming and outgoing types of fields that share the same coefficients $f_{jm\lambda}(k)$ by a superscript $|f\rangle^{\text{in}}$ or $|f\rangle^{\text{out}}$, versus the regular $|f\rangle$. Values of the corresponding scalar products are computed identically according to Eq. (28), (45), hence $\langle f|g \rangle = {}^{\text{in}}\langle f|g \rangle^{\text{in}} = {}^{\text{out}}\langle f|g \rangle^{\text{out}}$ for any coefficient functions f, g.

We can now see that our definition of basis fields $\boldsymbol{S}^{\text{in/out}}$ that incorporates an extra factor of $1/2$ when compared to its regular counterpart, and that differs from the usual approaches, follows from requiring the use of the same scalar product for regular, incoming and outgoing fields. Let us consider the number of photons in a regular pulse, which does not change with time. The decomposition of the regular pulse as $|f\rangle = |f\rangle^{\text{in}} + |f\rangle^{\text{out}}$ applies at all times, only that there are time periods where either $|f\rangle^{\text{out}}$ or $|f\rangle^{\text{in}}$ vanish. Notably, the total number of photons in the regular pulse $\langle f|f \rangle$ is equal to the number of photons absorbed ${}^{\text{in}}\langle f|f \rangle^{\text{in}}$ and also equal to the number of photons emitted ${}^{\text{out}}\langle f|f \rangle^{\text{out}}$.

2.4. On the convergence regions of some expansions

A discussion about the validity of particular kinds of field expansions is in order at this point. In the previous sections, we have identified the coefficient functions in expansions of electromagnetic fields as members of the Hilbert space. We argue here that, while some of those expansions do not converge at all space–time points, where more complicated expansions are needed, the coefficient functions contain sufficient information to recover the fields at all points outside material objects. The T-matrix and the S-matrix that we discuss in the next section are linear mappings between such coefficient functions.

Irregular basis fields are not defined in the whole space because they are singular at the origin $|\boldsymbol{r}| = 0$. However, in Eq. (97), the validity of the separation of a general regular pulse into the incoming and outgoing parts $\boldsymbol{E}_{\text{p}}^{\text{in}}(\boldsymbol{r}, t)$ and $\boldsymbol{E}_{\text{p}}^{\text{out}}(\boldsymbol{r}, t)$ depends on the pulse and may be restricted by a stronger condition than $|\boldsymbol{r}| > 0$. For example, a spatial translation of the pulse Eq. (97) by some distance a in any direction would decrease the region of validity of Eqs. (98)–(99) to points outside of the sphere with radius a, $|\boldsymbol{r}| > a$, while inside such sphere one must use another expansion branch featuring regular fields [38, Eq.(47ab)]. Similarly, the Lorentz boosted irregular electromagnetic field in Eq. (89) will not converge for all the $(\boldsymbol{r}, t)$ points, and an expansion with branches would also be then needed. A similar issue that arises in the T-matrix formalism is the validity of the expansion of the scattered field into only outgoing multipoles, similar to Eq. (99), which is strictly valid only outside the smallest sphere enclosing the scatterer. This issue, which can be addressed with more complicated expansions [4–10], also affects the S-matrix formalism, and the latter could also need branches to expand the incoming field, as in the case of the spatially translated pulse that we just discussed. However, even though expansions with branches are sometimes needed, it should be noted that the expansion coefficients of the far field are sufficient information to determine the field everywhere outside material objects. This follows from the fact that such coefficients determine the far field, which at its turn determines the field everywhere outside material objects [39, Theorems 6.9 and 6.10]. The work in [6] provides a clear illustration of this, since an accurate T-matrix of two nearby disks that grossly invade each other's smallest enclosing spheres can be computed using solely the positions and the T-matrices of each individual disk. Therefore, the expansion coefficient functions that constitute the Hilbert space, which determine the far fields, are sufficient information to recover the fields everywhere outside material objects, albeit potentially through relatively complicated expansions with e.g. several branches.

3. Polychromatic T-matrix and S-matrix

We now have all the necessary elements in place for defining the polychromatic T-matrix. Afterwards we will define the polychromatic S-matrix. Both operators contain the same information and are
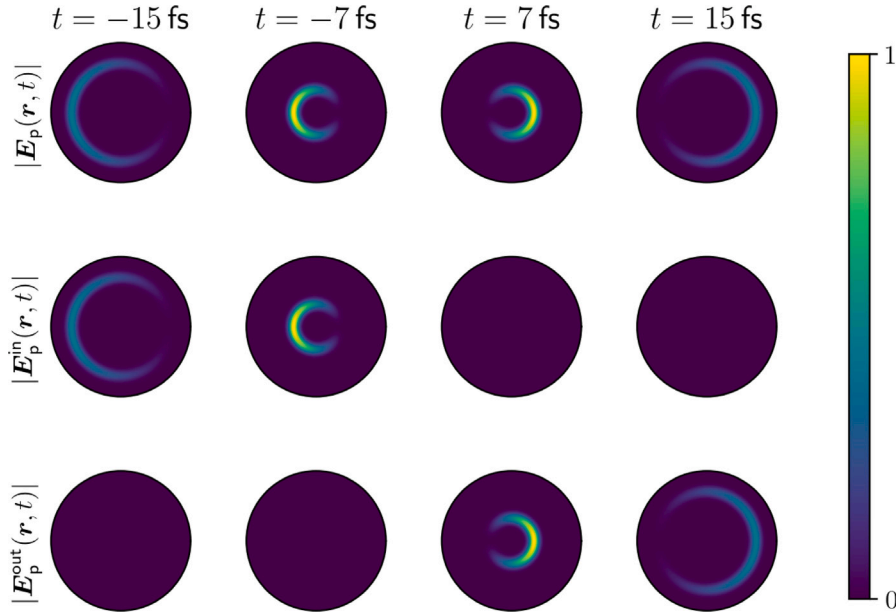
Fig. 1. Comparison of Gaussian pulses with center wavelength $\frac{2\pi}{k_0} = 400$ nm and Gaussian width $\Delta^{-1} = 300$ nm constructed as spectral superposition *with the same coefficients* of basis fields of different types: regular $\boldsymbol{R}_{jm\lambda}(k, \boldsymbol{r}, t)$ (top), incoming $\boldsymbol{S}^{in}_{jm\lambda}(k, \boldsymbol{r}, t)$ (middle) and outgoing $\boldsymbol{S}^{out}_{jm\lambda}(k, \boldsymbol{r}, t)$ (bottom), for $j = 1$, $m = 1$ and helicity $\lambda = 1$. Figures depict absolute values of the electric field in the zx-plane (z-axis points horizontally to the right, x-axis – vertically to the top) at four different points in time. The incoming pulse is computed to be identically zero after the end of its absorption in the origin, and is equal to the corresponding regular field for times before the start of its absorption. The outgoing pulse is computed to be identically zero before the start of its emission from the origin, and is equal to the corresponding regular field for times after the end of its emission.
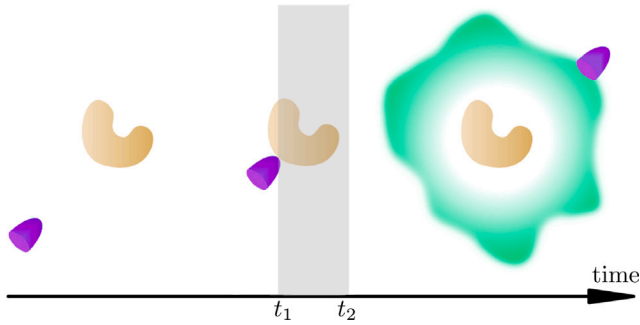
Fig. 2. An electromagnetic pulse interacts with a material object during a finite time (gray shade). The T-matrix is a linear operator in the Hilbert space of solutions of Maxwell equations that maps the incident fields (lilac) to the scattered fields (green). The light-matter interaction starts at $t = t_1$. Before t_1, causality forbids the existence of any scattered field. Time $t = t_2$ marks the end of the emission of the scattered field from the object.

bijectively connected, but they map different parts of the total electromagnetic field. The T-matrix connects the regular field, called incident field, with the irregular outgoing field, called scattered field. The S-matrix connects irregular incoming fields to irregular outgoing fields.

Let us start by considering the light-matter interaction picture in Fig. 2, where a light pulse interacts with a material object.

3.1. Polychromatic T-matrix

In the usual definition of the monochromatic T-matrix [40, Sec. 5.1], a time-harmonic field outside of the smallest sphere that encloses a localized electromagnetic scatterer can be written as a sum of the regular and outgoing multipoles

$$\boldsymbol{E}(k, \boldsymbol{r}, t) = e^{-ikct} \sum_{j=1}^{\infty} \sum_{m=-j}^{j} a_{jm} \, \boldsymbol{N}_{jm}(kr, \hat{\boldsymbol{r}}) + b_{jm} \, \boldsymbol{M}_{jm}(kr, \hat{\boldsymbol{r}})$$

$$+ e^{-ikct} \sum_{j=1}^{\infty} \sum_{m=-j}^{j} p_{jm} \, \boldsymbol{N}^{out}_{jm}(kr, \hat{\boldsymbol{r}}) + q_{jm} \, \boldsymbol{M}^{out}_{jm}(kr, \hat{\boldsymbol{r}}) \tag{102}$$

with the second equation valid for $r = |\boldsymbol{r}|$ larger than the radius of the smallest sphere enclosing the object. The first, regular part of Eq. (102) is called the incident field and the second, irregular part is called the scattered field.

In the case of a single monochromatic field, the usual monochromatic T-matrix is defined as the matrix that maps the coefficients of the incident and the scattered electromagnetic fields:

$$\begin{pmatrix} \vec{p} \\ \vec{q} \end{pmatrix} = T_u \begin{pmatrix} \vec{a} \\ \vec{b} \end{pmatrix}. \tag{103}$$

However, the most general linear scattering situation concerns interaction of a polychromatic field with an object. A total field in this case is a spectral superposition of monochromatic fields:

$$\boldsymbol{E}(k, \boldsymbol{r}, t) = \int_0^{\infty} dk \, e^{-ikct} \sum_{j=1}^{\infty} \sum_{m=-j}^{j} a_{jm}(k) \, \boldsymbol{N}_{jm}(kr, \hat{\boldsymbol{r}}) + b_{jm}(k) \, \boldsymbol{M}_{jm}(kr, \hat{\boldsymbol{r}})$$

$$+ \int_0^{\infty} dk \, e^{-ikct} \sum_{j=1}^{\infty} \sum_{m=-j}^{j} p_{jm}(k) \, \boldsymbol{N}^{out}_{jm}(kr, \hat{\boldsymbol{r}}) + q_{jm}(k) \, \boldsymbol{M}^{out}_{jm}(kr, \hat{\boldsymbol{r}}). \tag{104}$$

A principal difference to the monochromatic picture consists in the fact that a general linear connection between the incident and scattered field allows coupling of different frequencies. An example of a physical situation when this coupling is necessary is the relativistic scattering: a monochromatic beam that hits a moving object will produce a scattered field with components of several different frequencies.

Following the path suggested by the representation theory, we connect the electric field to the Hilbert space of solutions of Maxwell's equations by writing it in terms of the basis fields $\boldsymbol{R}_{jm\lambda}(k)$ and $\boldsymbol{S}^{out}_{jm\lambda}(k)$:

$$\boldsymbol{E}(\boldsymbol{r}, t) = \int_0^{\infty} dk \, k \sum_{\lambda=\pm 1} \sum_{j=1}^{\infty} \sum_{m=-j}^{j} f_{jm\lambda}(k) \, \boldsymbol{R}_{jm\lambda}(k, \boldsymbol{r}, t)$$

$$+ \int_0^{\infty} dk \, k \sum_{\lambda=\pm 1} \sum_{j=1}^{\infty} \sum_{m=-j}^{j} g_{jm\lambda}(k) \, \boldsymbol{S}^{out}_{jm\lambda}(k, \boldsymbol{r}, t), \tag{105}$$

or, equivalently

$$
\begin{aligned}
|f\rangle + |g\rangle^{\text{out}} = &\int_0^\infty dk\, k \sum_{\lambda=\pm 1} \sum_{j=1}^\infty \sum_{m=-j}^j f_{jm\lambda}(k)\, |kjm\lambda\rangle \\
&+ \int_0^\infty dk\, k \sum_{\lambda=\pm 1} \sum_{j=1}^\infty \sum_{m=-j}^j g_{jm\lambda}(k)\, |kjm\lambda\rangle^{\text{out}},
\end{aligned}
\tag{106}
$$

with coefficients that follow from Eqs. (105), (53), (87), and that, crucially, are compatible with the scalar product in Eq. (45):

$$
\begin{aligned}
f_{jm\lambda}(k) &= -\sqrt{\frac{\pi\epsilon_0}{2c\hbar}} \frac{(-i)^j}{k^2} \left(a_{jm}(k) + \lambda b_{jm}(k) \right) \\
g_{jm\lambda}(k) &= -\sqrt{\frac{2\pi\epsilon_0}{c\hbar}} \frac{(-i)^j}{k^2} \left(p_{jm}(k) + \lambda q_{jm}(k) \right).
\end{aligned}
\tag{107}
$$

In linear light-matter interactions the coefficients of the scattered field $g_{jm\lambda}(k)$ are linearly related to the coefficients of the incident field $f_{jm\lambda}(k)$. We define the polychromatic T-matrix as the linear operator mapping the regular incident field to the outgoing scattered field via

$$
|g\rangle^{\text{out}} = T|f\rangle
\tag{108}
$$

which implies for the coefficients

$$
\begin{aligned}
g_{j_1 m_1 \lambda_1}(k_1) &= \int_0^\infty dk_2\, k_2 \sum_{\lambda_2=\pm 1} \sum_{j_2=1}^\infty \sum_{m_2=-j_2}^{j_2} T_{j_2 m_2 \lambda_2}^{j_1 m_1 \lambda_1}(k_1, k_2) f_{j_2 m_2 \lambda_2}(k_2), \\
&\text{where } T_{j_2 m_2 \lambda_2}^{j_1 m_1 \lambda_1}(k_1, k_2) = {}^{\text{out}}\langle k_1 j_1 m_1 \lambda_1 | T | k_2 j_2 m_2 \lambda_2 \rangle.
\end{aligned}
\tag{109}
$$

Although the integration domain is unbounded, this does not introduce any computational limitations, since physical scatterers typically only interact in specific bounded frequency ranges. This allows a truncation of the integration domain when computing the scattered field.

3.2. Building frequency-diagonal polychromatic T-matrices from monochromatic T-matrices

Quite often, one considers scattering processes where frequencies do not change during light-matter interaction. Such processes can hence be described by T-matrices that are diagonal in frequency. Here we show how T-matrices that do not mix frequency are a special case of the polychromatic T-matrix, and provide the formula for building the polychromatic T-matrix from the usual monochromatic T-matrices.

Consider scattering of an incident field

$$
E_{\text{inc}}(\mathbf{r}, t) = \int dk\, e^{-ikct} \sum_{j=1}^\infty \sum_{m=-j}^j N_{jm}(kr, \hat{\mathbf{r}}) a_{jm}(k) + M_{jm}(kr, \hat{\mathbf{r}}) b_{jm}(k)
\tag{110}
$$

to a scattered field

$$
E_{\text{sc}}(\mathbf{r}, t) = \int dk\, e^{-ikct} \sum_{j=1}^\infty \sum_{m=-j}^j N_{jm}^{\text{out}}(kr, \hat{\mathbf{r}}) p_{jm}(k) + M_{jm}^{\text{out}}(kr, \hat{\mathbf{r}}) q_{jm}(k),
\tag{111}
$$

where the usual monochromatic T-matrices connect the coefficients at each frequency $\omega = kc$ as

$$
\begin{pmatrix} \vec{p}(k) \\ \vec{q}(k) \end{pmatrix} = T_u(k) \begin{pmatrix} \vec{a}(k) \\ \vec{b}(k) \end{pmatrix} = \begin{pmatrix} T_u^{NN}(k) & T_u^{NM}(k) \\ T_u^{ME}(k) & T_u^{MM}(k) \end{pmatrix} \begin{pmatrix} \vec{a}(k) \\ \vec{b}(k) \end{pmatrix}.
\tag{112}
$$

According to Eq. (109), the same scattering is realized by the following polychromatic T-matrix, which is diagonal in frequency (and written in

the helicity basis):

$$
\begin{aligned}
T_{j_2 m_2 \lambda_2}^{j_1 m_1 \lambda_1}(k_1, k_2) = \\
\frac{1}{k_2} \delta(k_1 - k_2) \Big(T_u^{NN}(k_2)_{j_2 m_2}^{j_1 m_1} \\
+ \lambda_1 T_u^{MN}(k_2)_{j_2 m_2}^{j_1 m_1} + \lambda_2 T_u^{NM}(k_2)_{j_2 m_2}^{j_1 m_1} + \lambda_1 \lambda_2 T_u^{MM}(k_2)_{j_2 m_2}^{j_1 m_1} \Big)
\end{aligned}
\tag{113}
$$

Eq. (113) follows from the decomposition of the fields in Eqs. (110)–(111), and from Eq. (107). We note that this formula already accounts for the extra factor of 2 that comes from the modified definition of the outgoing basis fields.

With the contents of this section, the monochromatic T-matrices $T_u(k)$ computed with the usual conventions by currently available formulas and computer codes can be easily re-used for computing the polychromatic T-matrix in the new conventions.

3.3. Polychromatic S-matrix

An equivalent description of scattering may be provided by the S-matrix formalism, which is based on the decomposition of the total electromagnetic field into the incoming and the outgoing fields [40, Eq. (5.47)]. Again, we generalize the monochromatic setting by considering the total field as the spectral superposition of monochromatic fields

$$
\begin{aligned}
E(\mathbf{r}, t) = &\int_0^\infty dk\, e^{-ikct} \sum_{j=1}^\infty \sum_{m=-j}^j \tilde{a}_{jm}(k) N_{jm}^{\text{in}}(kr, \hat{\mathbf{r}}) + \tilde{b}_{jm}(k) M_{jm}^{\text{in}}(kr, \hat{\mathbf{r}}) \\
&+ \int_0^\infty dk\, e^{-ikct} \sum_{j=1}^\infty \sum_{m=-j}^j \tilde{p}_{jm}(k) N_{jm}^{\text{out}}(kr, \hat{\mathbf{r}}) + \tilde{q}_{jm}(k) M_{jm}^{\text{out}}(kr, \hat{\mathbf{r}}).
\end{aligned}
\tag{114}
$$

Similarly to the previous section, we proceed by writing the total field Eq. (114) in terms of $S_{jm\lambda}^{\text{in/out}}$

$$
\begin{aligned}
E(\mathbf{r}, t) = &\int_0^\infty dk\, k \sum_{\lambda=\pm 1} \sum_{j=1}^\infty \sum_{m=-j}^j f_{jm\lambda}(k) S_{jm\lambda}^{\text{in}}(k, \mathbf{r}, t) \\
&+ \int_0^\infty dk\, k \sum_{\lambda=\pm 1} \sum_{j=1}^\infty \sum_{m=-j}^j h_{jm\lambda}(k) S_{jm\lambda}^{\text{out}}(k, \mathbf{r}, t),
\end{aligned}
\tag{115}
$$

or, equivalently

$$
\begin{aligned}
|f\rangle^{\text{in}} + |h\rangle^{\text{out}} = &\int_0^\infty dk\, k \sum_{\lambda=\pm 1} \sum_{j=1}^\infty \sum_{m=-j}^j f_{jm\lambda}(k)\, |kjm\lambda\rangle^{\text{in}} \\
&+ \int_0^\infty dk\, k \sum_{\lambda=\pm 1} \sum_{j=1}^\infty \sum_{m=-j}^j h_{jm\lambda}(k)\, |kjm\lambda\rangle^{\text{out}},
\end{aligned}
\tag{116}
$$

with coefficients that follow from Eq. (114) and Eq. (87), and that, crucially, are compatible with the scalar product in Eq. (45):

$$
\begin{aligned}
f_{jm\lambda}(k) &= -\sqrt{\frac{2\pi\epsilon_0}{c\hbar}} \frac{(-i)^j}{k^2} \left(\tilde{a}_{jm}(k) + \lambda \tilde{b}_{jm}(k) \right) \\
h_{jm\lambda}(k) &= -\sqrt{\frac{2\pi\epsilon_0}{c\hbar}} \frac{(-i)^j}{k^2} \left(\tilde{p}_{jm}(k) + \lambda \tilde{q}_{jm}(k) \right).
\end{aligned}
\tag{117}
$$

In linear light-matter interactions, the coefficients of the outgoing field $h_{jm\lambda}(k)$ are linearly related to the coefficients of the incoming field $f_{jm\lambda}(k)$. We define the polychromatic S-matrix as the linear operator mapping the incoming field to the outgoing field via

$$
|h\rangle^{\text{out}} = S|f\rangle^{\text{in}}
\tag{118}
$$

which implies for the coefficients

$$
h_{j_1 m_1 \lambda_1}(k_1) = \int_0^\infty dk_2\, k_2 \sum_{\lambda_2 = \pm 1} \sum_{j_2 = 1}^\infty \sum_{m_2 = -j_2}^{j_2} S_{j_2 m_2 \lambda_2}^{j_1 m_1 \lambda_1}(k_1, k_2) f_{j_2 m_2 \lambda_2}(k_2),
$$

$$
\text{where } S_{j_2 m_2 \lambda_2}^{j_1 m_1 \lambda_1}(k_1, k_2) = {}^{\text{out}}\langle k_1 j_1 m_1 \lambda_1 | S | k_2 j_2 m_2 \lambda_2 \rangle^{\text{in}}.
$$

(119)

The connection between the T-matrix and the S-matrix formalisms is determined by decompositions Eq. (105) and Eq. (115). We start with the T-matrix decomposition of total field into the incident and the scattered components and separate the regular part into the incoming and outgoing fields

$$
|f\rangle + |g\rangle^{\text{out}} = |f\rangle^{\text{in}} + |f\rangle^{\text{out}} + |g\rangle^{\text{out}}.
$$

(120)

This brings the total field to the decomposition that underlines the S-matrix formalism, implying

$$
S|f\rangle^{\text{in}} = |f\rangle^{\text{out}} + |g\rangle^{\text{out}} =: |h\rangle^{\text{out}},
$$

(121)

while the T-matrix maps the fields as

$$
T|f\rangle = |g\rangle^{\text{out}}.
$$

(122)

We see that in our convention the coefficients of the incident and of the incoming field are equal, namely $f_{jm\lambda}(k)$, and the coefficients of the outgoing field are connected to the coefficients of the incident and of the scattered fields via $h_{jm\lambda}(k) = f_{jm\lambda}(k) + g_{jm\lambda}(k)$.

Eq. (121) and Eq. (122) imply the connection between the T-matrix and the S-matrix as operators to be

$$
S|f\rangle^{\text{in}} = |f\rangle^{\text{out}} + T|f\rangle
$$

(123)

for arbitrary coefficients $f_{jm\lambda}(k)$. Numerically, when the elements of the T-matrix are known, the elements of the S-matrix may be computed via the simple relation

$$
S = \mathbb{1} + T,
$$

(124)

since the distinction between the incident, incoming and outgoing fields plays a role only when combining the coefficients with the corresponding basis elements to construct the physical field $E(r, t)$.

Eq. (124) also allows to straightforwardly obtain results identical to of Section 3.2 for the case of the frequency-diagonal S-matrix.

We note that the connection in Eq. (124) differs from a more common formula

$$
S_u = \mathbb{1} + 2T_u,
$$

(125)

where the subscript 'u' stands for the usual way of defining basis states. The reason lies in the way our basis fields $S_{jm\lambda}^{\text{in/out}}$ are defined, namely via substituting spherical Bessel functions $j_L(kr)$ in $R_{jm\lambda}$ by spherical Hankel functions halved $h_L^{\text{in/out}}(kr)/2$. In the usual approach, however, the irregular vector spherical functions $M_{jm}^{\text{in/out}}$ and $N_{jm}^{\text{in/out}}$ are defined by substituting spherical Bessel functions by spherical Hankel functions without division by 2.

While the T-matrix in our convention is larger than the usual one by the factor of two, the S-matrix is identical in both conventions, because incoming and outgoing basis fields have been changed in the same way, and therefore numerical values of the S-matrix elements ${}^{\text{out}}\langle k_1 m_1 \lambda_1 | S | k_2 j_2 m_2 \lambda_2 \rangle^{\text{in}}$ do not change.

4. Transfer of energy and momentum from a light pulse to a Si sphere

In the following example we illustrate how one can use the polychromatic T-matrix method for the computation of the transfer of energy and momentum between an electromagnetic pulse and a silicon sphere. The silicon sphere is represented as a polychromatic T-matrix that is diagonal in frequency, as per Eq. (113).

The scalar product in Eq. (28) or Eq. (45) allows one to compute fundamental physical quantities, such as energy, momentum, and angular momentum carried by electromagnetic field $|f\rangle$:

$$
\langle \Gamma \rangle = \langle f | \Gamma | f \rangle,
$$

(126)

where Γ is the Hermitian operator of the corresponding physical quantity: generator of time translations $cP^0 = H$ for energy, generators for spatial translations P_α ($\alpha = x, y, z$) for linear momentum, and generators of rotations J_α ($\alpha = x, y, z$) for angular momentum. If the scattering process is subject to a conservation law, then the difference between the quantities contained in incoming and outgoing fields is equal to the amount of the quantity transferred to or extracted from the object. For the purpose of computing this difference it is most convenient to describe scattering in terms of the S-matrix. Given the incoming field $|f\rangle^{\text{in}}$ and the outgoing field $|h\rangle^{\text{out}} = S|f\rangle^{\text{in}}$, the transferred amount $\langle \Delta \Gamma \rangle$ is [20, Eq. (3)]

$$
\langle \Delta \Gamma \rangle = {}^{\text{in}}\langle f | \Gamma | f \rangle^{\text{in}} - {}^{\text{out}}\langle h | \Gamma | h \rangle^{\text{out}}
$$

$$
= {}^{\text{in}}\langle f | \Gamma - S^\dagger \Gamma S | f \rangle^{\text{in}},
$$

(127)

or, using Eq. (123), in terms of the T-matrix

$$
\langle \Delta \Gamma \rangle = -{}^{\text{out}}\langle f | \Gamma T | f \rangle - \langle f | T^\dagger \Gamma | f \rangle^{\text{out}} - \langle f | T^\dagger \Gamma T | f \rangle.
$$

(128)

The superscripts signify the correct types of the fields, however, as previously discussed in Sec. 2.3.2, the values of the scalar products are independent of these types.

We illustrate the transfer of quantities with a left-handed ($\lambda = +1$) circularly polarized pulse with Gaussian profile in time, described by the wave function at positive $\cos \theta$ as

$$
f_+(k) = A\, e^{i\phi} \cos\theta (1 + \cos\theta)\, e^{-(k-k_0)^2 \Delta_t^2 c^2 / 2}\, e^{-k^2(1 - \cos^2\theta)\Delta_\rho^2 / 2},
$$

(129)

$$
f_-(k) = 0,
$$

(130)

and set $f_\lambda(k) = 0$ for $\cos\theta < 0$. The angles θ and ϕ are the polar and azimuthal angles of k respectively. We choose time width of the pulse $\Delta_t = 10$ fs, spacial parameter $\Delta_\rho = 1$ μm, the central wavelength $\frac{2\pi}{k_0} = 380$ nm. The constructed pulse is focused along the z-direction, such that the values of the coefficients that correspond to polar angles with $\cos\theta < 0.975$ are vanishingly small. We will use this fact for more efficient discretization of the integrals in the plane wave basis.

We set the constant $A = 6.5 \times 10^{10}$ nm to fix the energy of the pulse to 1 mJ:

$$
\langle f | H | f \rangle = \sum_{\lambda = \pm 1} \int \frac{d^3 k}{k} |f_\lambda(k)|^2 c\hbar k = 1.0 \times 10^{-3} \text{ J},
$$

(131)

which is a concrete realization of Eq. (126). Here and later the integration over k is truncated to the region $15.3\ \mu\text{m}^{-1} \leq k \leq 17.8\ \mu\text{m}^{-1}$. Outside of this region the pulse has negligible frequency content (see the corresponding profile on Fig. 3(a) in green). The integral is computed as a Riemann sum with the number of equidistant points $N_k = 150$. The numerical integration over directions of the wave vector is truncated to $\int_0^{2\pi} d\phi \int_{0.975}^1 d(\cos\theta)$ with discretization $N_\phi = 200$ and $N_{\cos\theta} = 300$. The summation over j is truncated up to the multipole order $j_{\max} = 8$, above which the T-matrix elements are negligible in the relevant frequency band.

Similarly, the momentum in z-direction that is contained in the pulse can be computed via

$$
\langle f | P_z | f \rangle = \sum_{\lambda = \pm 1} \int \frac{d^3 k}{k} |f_\lambda(k)|^2 \hbar k \cos\theta = 3.3 \times 10^{-12} \text{ kg m s}^{-1}.
$$

(132)

Now let us consider interaction of the defined pulse with a silicon sphere of radius 100 nm located in the origin of the reference frame.
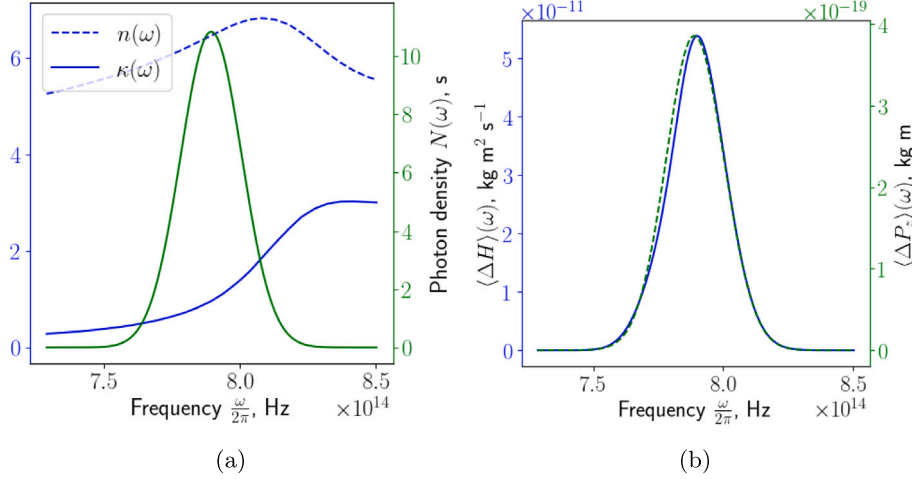
Fig. 3. (a) Refractive index $n(\omega)$ and extinction coefficient $\kappa(\omega)$ of Silicon as a function of frequency (blue) together with the photon density with respect to the frequency of the incident field (green). (b) Transfer of energy from the pulse to the object per frequency (blue), together with the transfer of linear momentum in z-direction from the pulse to the object per frequency (green). Integrals of the functions provide the total transferred quantity.

The spectral content of the incident pulse in terms of its photon density w.r.t. angular frequency $\omega = kc$:

$$N(\omega) := \frac{\omega}{c^2} \sum_{\lambda=\pm 1} \int_0^{2\pi} d\phi \int_{-1}^1 d(\cos\theta) |f_\lambda(\boldsymbol{k})|^2 \tag{133}$$

is illustrated on top of the optical parameters of the silicon [41] on Fig. 3(a).

We compute the transfer of the energy and of the momentum in the angular momentum basis, for which one requires the infinitesimal versions of the transformation laws Eq. (70)–(71), which read

$$H f_{jm\lambda}(k) = \hbar c k f_{jm\lambda}(k) \tag{134}$$

$$P_z f_{jm\lambda}(k) =$$

$$\hbar k \sqrt{2j+1}(-1)^{m-\lambda} \sum_{j'=j-1}^{j+1} \sqrt{2j'+1} \begin{pmatrix} j & j' & 1 \\ -m & m & 0 \end{pmatrix} \begin{pmatrix} j & j' & 1 \\ -\lambda & \lambda & 0 \end{pmatrix} f_{j'm\lambda}(k), \tag{135}$$

where $\begin{pmatrix} j_1 & j_2 & j_3 \\ m_1 & m_2 & m_3 \end{pmatrix}$ are the Wigner 3-j symbols. We generate the T-matrix of the sphere at different wavenumbers for $j_{\max} = 8$ with the `treams` python package [25,26], which is publicly available at https://github.com/tfp-photonics/treams, and use Eq. (128) to get the transfer of energy and momentum to the object:

$$\langle \Delta H \rangle = 9.15 \times 10^{-6} \text{ J} \tag{136}$$

$$\langle \Delta P_z \rangle = 6.80 \times 10^{-14} \text{ kg m s}^{-1}. \tag{137}$$

A more specific information on the transfer is provided in Fig. 3(b), where the density of transferred quantity with respect to the frequency is plotted for both energy $\langle \Delta H \rangle(\omega)$ and momentum $\langle \Delta P_z \rangle(\omega)$ transfer. The amounts of total transfer are connected to the corresponding densities as

$$\langle \Delta H \rangle = \int_0^\infty d\omega \, \langle \Delta H \rangle(\omega) \tag{138}$$

$$\langle \Delta P_z \rangle = \int_0^\infty d\omega \, \langle \Delta P_z \rangle(\omega). \tag{139}$$

This method differs from alternative approaches that make use of the Maxwell's stress tensor [42]. Instead, we employ the scalar product formula Eq. (45), which enables us to achieve accurate results while highlighting the underlying group-theoretical principles.

4.1. Validation of results

We validate some of our results by computing the energy transfer via the well-known formula for the energy contained in an electromagnetic field

$$E_{\text{em}} = \frac{\epsilon_0}{2} \int d^3\boldsymbol{r} \, |\boldsymbol{\mathcal{E}}(\boldsymbol{r},t)|^2 + |c\boldsymbol{\mathcal{B}}(\boldsymbol{r},t)|^2, \tag{140}$$

which can be alternatively written in terms of Riemann–Silberstein vectors using Eqs. (4) and (13)

$$E_{\text{em}} = \epsilon_0 \int d^3\boldsymbol{r} \, |\boldsymbol{F}_+(\boldsymbol{r},t) + \boldsymbol{F}_-^*(\boldsymbol{r},t)|^2. \tag{141}$$

Knowing the coefficients of the incident $f_{jm\lambda}(k)$ and the scattered field $g_{jm\lambda}(k)$, the corresponding incoming and outgoing coefficients read (see Section 3.3)

$$f_{jm\lambda}^{\text{in}}(k) = f_{jm\lambda}(k) \tag{142}$$

$$f_{jm\lambda}^{\text{out}}(k) = f_{jm\lambda}(k) + g_{jm\lambda}(k). \tag{143}$$

Combining them with the incoming and outgoing basis fields in Eq. (84), and taking into account Eq. (13), gives the required electromagnetic fields in $(\boldsymbol{r},t)$-domain:

$$\boldsymbol{F}_\lambda^{\text{in/out}}(\boldsymbol{r},t) = \sqrt{2} \int_0^\infty dk \, k \sum_{j=1}^\infty \sum_{m=-j}^j \sum_{\lambda=\pm 1} f_{jm\lambda}^{\text{in/out}}(k) \boldsymbol{S}_{jm\lambda}^{\text{in/out}}(k,\boldsymbol{r},t). \tag{144}$$

As in the previous section, the wavenumber integration can be truncated to the region $15.3 \text{ μm}^{-1} \le k \le 17.8 \text{ μm}^{-1}$. Since the scatterer does not interact with the parts of the field with $j > j_{\max} = 8$, higher multipolar component of the outgoing field will be the same as the corresponding components of the incoming field. Hence, the difference of their carried energy will be zero, and they do not contribute to the energy transfer. This allows us to focus on the transfer of energy due to $j \le j_{\max} = 8$ components of the field.

The energy density of the $j \le 8$ components of incoming and the outgoing fields at specific times is depicted in Fig. 4

Numerical integration of Eq. (141) is conducted in spherical coordinates as a Riemann sum in $r \in [0,55]$μm, $\theta \in [0,\pi]$ and $\phi \in [0,2\pi]$, for $N_r = 250$, $N_\theta = 500$ and $N_\phi = 201$ equidistant points, preceded by the integration of Eq. (144) over $N_k = 150$ equidistant points. The incoming field is considered at time $t = -150$ fs and the outgoing at $t = 150$ fs. The resulting energy difference is

$$E_{\text{em}}^{\text{in}} - E_{\text{em}}^{\text{out}} = 2.49417 \times 10^{-4}\text{J} - 2.40224 \times 10^{-4}\text{J} = 9.1929 \times 10^{-6}\text{J}, \tag{145}$$
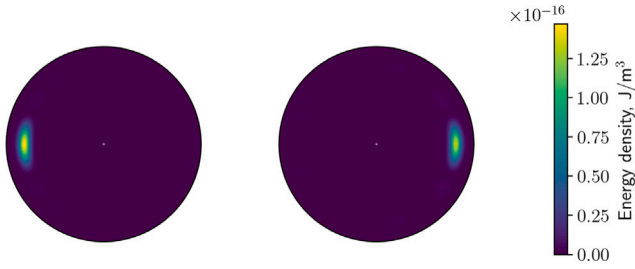
Fig. 4. Energy density of the incoming (left) and the outgoing (right) parts of the total field for multipole order up to $j_{max} = 8$, plotted in the zx-plane with horizontal z-axis and vertical x-axis. The radial dimension of the plot is 55 µm, the incoming field is plotted at time -150 fs and the outgoing field at time 150 fs. The white circle in the middle represents the silicon sphere.

which is in very good agreement with the value given by the scalar product approach 9.1503×10^{-6} J. The small difference can be attributed to numerical noise.

5. Conclusions

In this work, we have generalized the T-matrix method to the polychromatic setting by exploiting the connection between electromagnetism and the theory of group representations. This extension broadens the range of scenarios that can be accurately modeled and studied using the T-matrix method, allowing for a more comprehensive understanding of electromagnetic scattering phenomena.

Through the introduction of a novel convention for electromagnetic basis fields, which possess the distinctive property of transforming according to specific unitary representations of the Poincaré group of special relativity, we have achieved the unification of incoming, outgoing, and regular fields, enabling the use of the same scalar product in all cases. Additionally, we have shown that incoming, outgoing and regular fields transform identically under Lorentz boosts, and derived the closed form matrix element of the Lorentz boost of the polychromatic T-matrix, providing a solid theoretical foundation for investigating the interaction of electromagnetic fields with relativistically moving objects.

To demonstrate the practical implications of our research, we have conducted numerical computations of the transfer of quantities such as energy and momentum from an electromagnetic pulse to a silicon sphere. These results serve as concrete examples of the applicability of the proposed enhancements to the T-matrix method.

By refining the T-matrix method and expanding its capabilities, we provide researchers with valuable tools for advancements in the field of electromagnetic scattering.

CRediT authorship contribution statement

Maxim Vavilin: Conceptualization, Investigation, Methodology, Validation, Visualization, Writing – original draft. **Ivan Fernandez-Corbaton:** Conceptualization, Investigation, Methodology, Writing – review & editing.

Declaration of competing interest

The authors declare that they have no known competing financial interests or personal relationships that could have appeared to influence the work reported in this paper.

Data availability

The code to reproduce numerical results can be accessed via https://www.waves.kit.edu/downloads/CRC1173_Preprint_2023-16_Codes.zip.

Appendix A. The representation of the vector potential

The transverse part of the vector potential determines the transverse electric field

$$E(r, t) = -\frac{\partial A^{\perp}(r, t)}{\partial t}, \tag{146}$$

independently of the gauge [43, Eq. B.26]. In the wave vector space we have hence $\bar{A}^{\perp}(k) = \frac{-i\bar{E}(k)}{ck}$, and the decomposition equivalent to Eq. (10) reads

$$A^{\perp}(r, t) = \sqrt{\frac{\hbar}{c\epsilon_0}} \frac{1}{\sqrt{2}} \frac{-i}{\sqrt{(2\pi)^3}} \sum_{\lambda = \pm 1} \int \frac{d^3 k}{k} f_{\lambda}(k) \, e_{\lambda}(\hat{k}) \, e^{i(k \cdot r - ckt)}, \tag{147}$$

where the coefficients of the decomposition $f_{\lambda}(k)$ are the same as the ones of the corresponding electric field. Since one should keep the invariant measure $\frac{d^3 k}{k}$, the decomposition in Eq. (147) induces a definition of plane waves for the vector potential that differs from one of the electric plane waves by the factor of ik/c:

$$Q_{\lambda}^{A^{\perp}}(k, r, t) = -i\sqrt{\frac{\hbar}{c\epsilon_0}} \frac{1}{\sqrt{2}} \frac{1}{\sqrt{(2\pi)^3}} \, e_{\lambda}(\hat{k}) e^{-ickt} e^{ik \cdot r}. \tag{148}$$

Vector potential plane waves obey the same transformation rules Eqs. (16)–(18) and Eq. (19), with an exception of time reversal, where the difference in the imaginary unit i introduces an extra factor of (-1) to the right hand side of Eq. (20). The presence of $\frac{\partial}{\partial t}$ in Eq. (146) already announces this difference in time-reversal transformation properties. Also the factor of k difference exactly compensates for the different way that $A^{\perp}(r, t)$ and $E(r, t)$ transform under Lorentz boosts, namely as the space component of a four-vector, and as the space–time component of an anti-symmetric tensor, respectively.

Appendix B. Lorentz boosts in the (r, t) representation of fields

Active Lorentz boosts relativistically describe an object moving with a uniform velocity v. A 4-vector in Minkowski space–time is transformed under a Lorentz boosts in the z-direction via

$$x^{\mu} = \begin{pmatrix} ct \\ x^1 \\ x^2 \\ x^3 \end{pmatrix} \mapsto L_z(\xi)^{\mu}{}_{\nu} x^{\nu} = \begin{pmatrix} \cosh(\xi) & 0 & 0 & \sinh(\xi) \\ 0 & 1 & 0 & 0 \\ 0 & 0 & 1 & 0 \\ \sinh(\xi) & 0 & 0 & \cosh(\xi) \end{pmatrix} \begin{pmatrix} ct \\ x^1 \\ x^2 \\ x^3 \end{pmatrix}, \tag{149}$$

with rapidity $\xi = \tanh(v/c)$. A Lorentz boost in an arbitrary direction can be written as a composition the boost in the z-direction with spatial rotations:

$$L_{\hat{n}}(\xi) = R(\phi, \theta, 0) L_z(\xi) R^{-1}(\phi, \theta, 0). \tag{150}$$

where the direction of the boost $\hat{n}$ is parametrized by polar angle $\theta = \arccos(k_z/|k|)$ and azimuthal angle $\phi = \text{atan2}(k_y, k_x)$, and the rotations R are parametrized with Euler angles.

In the specific case of a massless 4-wave vector k^{μ} with $k^0 = |k|$ the transformation in the z-direction reads

$$k^{\mu} = \begin{pmatrix} |k| \\ k^1 \\ k^2 \\ k^3 \end{pmatrix} \mapsto \begin{pmatrix} \cosh(\xi)|k| + \sinh(\xi)k^3 \\ k^1 \\ k^2 \\ \sinh(\xi)|k| + \cosh(\xi)k^3 \end{pmatrix}. \tag{151}$$

and the transformed angles of the wave vector satisfy

$$\tilde{\phi} = \phi \tag{152}$$

$$\cos(\tilde{\theta}) = \frac{\cos(\theta)\cosh(\xi) + \sinh(\xi)}{\cosh(\xi) + \cos(\theta)\sinh(\xi)} \tag{153}$$

$$\sin(\tilde{\theta}) = \frac{\sin(\theta)}{\cosh(\xi) + \cos(\theta)\sinh(\xi)}. \tag{154}$$

An active Lorentz boost transformation of real-valued electromagnetic fields, which we distinguish it from the complex fields by a different font, is defined as [35, Sec.11.10]

$$\widetilde{\mathcal{E}}(r,t) = \gamma \mathcal{E}(\tilde{r}, \tilde{t}) - \gamma v \times \mathcal{B}(\tilde{r}, \tilde{t}) - \frac{\gamma^2 v}{(\gamma+1)c^2} v \cdot \mathcal{E}(\tilde{r}, \tilde{t}) \tag{155}$$

$$\widetilde{\mathcal{B}}(r,t) = \gamma \mathcal{B}(\tilde{r}, \tilde{t}) + \frac{1}{c^2}\gamma v \times \mathcal{E}(\tilde{r}, \tilde{t}) - \frac{\gamma^2 v}{(\gamma+1)c^2} v \cdot \mathcal{B}(\tilde{r}, \tilde{t}) \tag{156}$$

with inversely transformed space–time point $\begin{pmatrix} c\tilde{t} \\ \tilde{r} \end{pmatrix} = L^{-1}(\xi)\begin{pmatrix} ct \\ r \end{pmatrix}$ and $\gamma = (1 - v^2/c^2)^{-1/2}$. The passive version of the Lorentz boost, i.e. the boost of the reference frame instead of the field, differs from Eqs. (155)–(156) by the substitution $v \to -v$ and should not be confused with the active version.

One can show that the corresponding Riemann–Silberstein vectors in Eq. (11) transform under active Lorentz boosts as

$$\widetilde{F}_\lambda(r,t) = \gamma F_\lambda(\tilde{r}, \tilde{t}) + \frac{i\lambda\gamma}{c} v \times F_\lambda(\tilde{r}, \tilde{t}) - \frac{\gamma^2 v}{(\gamma+1)c^2} v \cdot F_\lambda(\tilde{r}, \tilde{t}). \tag{157}$$

Appendix C. Transformation properties of $|k\lambda\rangle$

Here we derive the transformation laws for plane waves

$$Q_\lambda(k,r,t) := \frac{1}{\sqrt{2}} \frac{1}{\sqrt{(2\pi)^3}} \sqrt{\frac{c\hbar}{\epsilon_0}} \, k \, e_\lambda(\hat{k}) e^{-ikct} e^{ik\cdot r} \tag{158}$$

under the actions of the full Poincaré group. The transformation laws for the general electromagnetic field in the (r,t)-representation are well-known, and we show how they can be equivalently formulated in the (k,λ)-domain as a unitary transformation with respect to the scalar product of Eq. (28).

C.1. Translations

Active spatio-temporal translations of electric field by $a^\mu = (a, a^0)$ are defined with

$$\widetilde{E}(r,t) = E(r - a, t - a^0). \tag{159}$$

Then, using Eq. (10)

$$\widetilde{E}(r,t) = \frac{1}{\sqrt{2}} \frac{1}{\sqrt{(2\pi)^3}} \sqrt{\frac{c\hbar}{\epsilon_0}} \sum_{\lambda=\pm1} \int \frac{d^3 k}{k} f_\lambda(k) \, k \, e_\lambda(\hat{k}) e^{ik_\mu(x^\mu - a^\mu)}$$
$$= \frac{1}{\sqrt{2}} \frac{1}{\sqrt{(2\pi)^3}} \sqrt{\frac{c\hbar}{\epsilon_0}} \sum_{\lambda=\pm1} \int \frac{d^3 k}{k} f_\lambda(k) \, p \, e_\lambda(\hat{k}) e^{ik_\mu x^\mu} e^{-ik_\mu a^\mu} \tag{160}$$

For the plane wave this implies the transformation law

$$Q_\lambda(k, r - a, t - a^0) = \frac{1}{\sqrt{2}} \frac{1}{\sqrt{(2\pi)^3}} \sqrt{\frac{c\hbar}{\epsilon_0}} \, k \, e_\lambda(\hat{k}) e^{ik_\mu(x^\mu - a^\mu)}$$
$$= Q_\lambda(k,r,t) e^{-ik_\mu a^\mu} \tag{161}$$

which corresponds to Eq. (16).

C.2. Rotations

Active rotations of electric field by Euler angles (α, β, γ), $R(\alpha, \beta, \gamma) = R_z(\alpha)R_y(\alpha)R_z(\gamma)$ are defined in (r,t)-domain as [35, Sec. 6.10]

$$\widetilde{E}(r,t) = R(\alpha, \beta, \gamma) \, E(R^{-1}(\alpha, \beta, \gamma)r, t) \tag{162}$$

where arguments are transformed inversely with respect to the vectorial part. Here and after we use letter R as an abstract operator to describe rotations, and its action depends on the concrete representation of the element that it acts upon. Vectors in the physical three-dimensional space are rotated according to the usual representation of rotations in space, while the polarization vectors $e_\sigma(\hat{k})$ are rotated via the Wigner matrix $D^1(\alpha, \beta, \gamma)$ [31, Eq. (76)]:

$$R(\alpha, \beta, \gamma)e_\sigma(\hat{k}) = \sum_{\mu=-1,0,1} e_\mu(\hat{k}) \, D^1_{\mu\sigma}(\alpha, \beta, \gamma), \tag{163}$$

a special case of which is

$$R_z(\psi)e_\lambda(\hat{z}) = e_\lambda(\hat{z})e^{-i\lambda\psi}. \tag{164}$$

Eq. (163) also allows to find the polarization vector pointing in a general (ϕ, θ)-direction in terms of the helicity basis at $\hat{z}$:

$$e_\lambda(\hat{k}) = R(\phi, \theta, 0)e_\lambda(\hat{z}) = \sum_{\mu=-1,0,1} e_\mu(\hat{z}) \, D^1_{\mu\lambda}(\phi, \theta, 0). \tag{165}$$

Application of the rotation law Eq. (162) to the electric field decomposition Eq. (10) gives

$$\widetilde{E}(r,t) = \frac{1}{\sqrt{2}} \frac{1}{\sqrt{(2\pi)^3}} \sqrt{\frac{c\hbar}{\epsilon_0}}$$
$$\times \sum_{\lambda=\pm1} \int \frac{d^3 k}{k} f_\lambda(k) \, k \, R(\alpha, \beta, \gamma)e_\lambda(\hat{k}) \, e^{-ikct} e^{ik\cdot(R^{-1}(\alpha,\beta,\gamma)r)}. \tag{166}$$

First, we rewrite the vectorial part as

$$R(\alpha, \beta, \gamma)e_\lambda(\hat{k}) = R(\alpha, \beta, \gamma)R(\phi, \theta, 0)e_\lambda(\hat{z})$$
$$= R(\tilde{\phi}, \tilde{\theta}, \psi)e_\lambda(\hat{z}), \tag{167}$$

where the rotation by angles $(\tilde{\phi}, \tilde{\theta}, \psi)$ realizes the equivalent action to the of two consecutive rotations: $R(\alpha, \beta, \gamma)R(\phi, \theta, 0) = R(\tilde{\phi}, \tilde{\theta}, \psi)$. Next, we separate the rotation $R(\tilde{\phi}, \tilde{\theta}, \psi) = R(\tilde{\phi}, \tilde{\theta}, 0)R_z(\psi)$ and use Eqs. (164)–(165) to simplify the vectorial part to

$$R(\alpha, \beta, \gamma)e_\lambda(\hat{k}) = e_\lambda(\hat{\tilde{k}})e^{-i\lambda\psi}, \tag{168}$$

with $\tilde{\theta}$ and $\tilde{\phi}$ being the polar and the azimuthal angles of the rotated wave vector $\tilde{k}$.

Transformed scalar part satisfies

$$e^{ik\cdot(R^{-1}(\alpha,\beta,\gamma)r)} = e^{i(R(\alpha,\beta,\gamma)k)\cdot r} = e^{i\tilde{k}\cdot r}, \tag{169}$$

which together with the fact $|k| = |\tilde{k}|$ brings Eq. (166) to

$$\widetilde{E}(r,t) = \frac{1}{\sqrt{2}} \frac{1}{\sqrt{(2\pi)^3}} \sqrt{\frac{c\hbar}{\epsilon_0}} \sum_{\lambda=\pm1} \int \frac{d^3 k}{k} f_\lambda(k) \, \tilde{k} \, e_\lambda(\hat{\tilde{k}})e^{-i\lambda\psi} \, e^{-i\tilde{k}ct} e^{i\tilde{k}\cdot r}$$
$$= \sum_{\lambda=\pm1} \int \frac{d^3 k}{k} f_\lambda(k) \, Q_\lambda(\tilde{k}, r, t)e^{-i\lambda\psi}. \tag{170}$$

The last equation implies the required Eq. (17):

$$Q_\lambda(k, r, t) \mapsto Q_\lambda(\tilde{k}, r, t)e^{-i\lambda\psi}. \tag{171}$$

C.3. Parity

Electric field transforms under parity as [35, Sec. 6.10]

$$E'(r,t) = -E(-r,t). \tag{172}$$

Then, using decomposition Eq. (10)

$$E'(r,t) = -\frac{1}{\sqrt{2}} \frac{1}{\sqrt{(2\pi)^3}} \sqrt{\frac{c\hbar}{\epsilon_0}} \sum_{\lambda=\pm1} \int \frac{d^3 k}{k} f_\lambda(k) \, k \, e_\lambda(\hat{k}) \, e^{ik\cdot(-r)} \, e^{-ikct}. \tag{173}$$

For the plane wave this implies the transformation law

$$Q_\lambda(k, r, t) \mapsto -Q_\lambda(k, -r, t)$$
$$= -\frac{1}{\sqrt{2}} \frac{1}{\sqrt{(2\pi)^3}} \sqrt{\frac{c\hbar}{\epsilon_0}} \, k \, e_\lambda(\hat{k})e^{-ikct} e^{ik\cdot(-r)}. \tag{174}$$

Using the definition Eq. (6) one can directly check that

$$-e_\lambda(\hat{k}) = e_{-\lambda}(-\hat{k}), \tag{175}$$

hence one arrives at

$$\boldsymbol{Q}_\lambda(\boldsymbol{k}, \boldsymbol{r}, t) \mapsto \boldsymbol{Q}_{-\lambda}(-\boldsymbol{k}, \boldsymbol{r}, t) \tag{176}$$

which corresponds to Eq. (19).

C.4. Time reversal

Time reversal of real-valued fields is defined as [35, Sec. 6.10]

$$\mathcal{E}'(\boldsymbol{r}, t) = \mathcal{E}(\boldsymbol{r}, -t). \tag{177}$$

For the complex representation of electromagnetic field Eq. (3) this implies

$$\boldsymbol{E}(\boldsymbol{r}, t) = \frac{1}{\sqrt{2\pi}} \int_0^\infty dk \, e^{-ikct} \, \tilde{\boldsymbol{E}}(\boldsymbol{r}, k) \mapsto \frac{1}{\sqrt{2\pi}} \int_0^\infty dk \, e^{-ikct} \, \tilde{\boldsymbol{E}}(\boldsymbol{r}, k)^*. \tag{178}$$

Then, using decomposition Eq. (10) the time-reversed field can be written as

$$\boldsymbol{E}'(\boldsymbol{r}, t) = \frac{1}{\sqrt{2}} \frac{1}{\sqrt{(2\pi)^3}} \sqrt{\frac{c\hbar}{\epsilon_0}} \sum_{\lambda=\pm 1} \int \frac{d^3\boldsymbol{k}}{k} \left[f_\lambda(\boldsymbol{k}) \, k \, \boldsymbol{e}_\lambda(\hat{\boldsymbol{k}}) \, e^{i\boldsymbol{k}\cdot\boldsymbol{r}} \right]^* e^{-ikct}$$

$$= \frac{1}{\sqrt{2}} \frac{1}{\sqrt{(2\pi)^3}} \sqrt{\frac{c\hbar}{\epsilon_0}} \sum_{\lambda=\pm 1} \int \frac{d^3\boldsymbol{k}}{k} f_\lambda^*(\boldsymbol{k}) \, k \, \boldsymbol{e}_\lambda(-\hat{\boldsymbol{k}}) \, e^{i(-\boldsymbol{k})\cdot\boldsymbol{r}} e^{-ikct}. \tag{179}$$

Using Eq. (6) one can straightforwardly check that

$$\boldsymbol{e}_\lambda^*(\hat{\boldsymbol{k}}) = \boldsymbol{e}_\lambda(-\hat{\boldsymbol{k}}), \tag{180}$$

hence the plane waves transform as

$$\boldsymbol{Q}_\lambda(\boldsymbol{k}, \boldsymbol{r}, t) \mapsto \boldsymbol{Q}_\lambda(-\boldsymbol{k}, \boldsymbol{r}, t). \tag{181}$$

which corresponds to Eq. (20). The equivalent transformation of the coefficients $f_\lambda(\boldsymbol{k})$ involves complex-conjugation

$$f_\lambda(\boldsymbol{k}) \mapsto f_\lambda^*(-\boldsymbol{k}), \tag{182}$$

which reflects the fact that time reversal is represented anti-unitarily.

Appendix D. Parity and time reversal for $|kjm\lambda\rangle$

For completeness, we provide here the transformation laws of the relevant angular momentum basis vector fields

$$\boldsymbol{R}_{jm\lambda}(k, \boldsymbol{r}, t) = \frac{1}{\sqrt{\epsilon_0 \hbar c}} \frac{k \, e^{-ikct}}{\sqrt{\pi} \sqrt{2j+1}} \sum_{L=j-1}^{j+1} \sqrt{2L+1} \, i^L j_L(kr) \, C_{L0,1\lambda}^{j\lambda} \boldsymbol{Y}_{jm}^L(\hat{\boldsymbol{r}}) \tag{183}$$

$$\boldsymbol{S}_{jm\lambda}^{\text{out}}(k, \boldsymbol{r}, t) = \frac{1}{2} \frac{1}{\sqrt{\epsilon_0 \hbar c}} \frac{k \, e^{-ikct}}{\sqrt{\pi} \sqrt{2j+1}} \sum_{L=j-1}^{j+1} \sqrt{2L+1} \, i^L h_L^{\text{out}}(kr) \, C_{L0,1\lambda}^{j\lambda} \boldsymbol{Y}_{jm}^L(\hat{\boldsymbol{r}}) \tag{184}$$

$$\boldsymbol{S}_{jm\lambda}^{\text{in}}(k, \boldsymbol{r}, t) = \frac{1}{2} \frac{1}{\sqrt{\epsilon_0 \hbar c}} \frac{k \, e^{-ikct}}{\sqrt{\pi} \sqrt{2j+1}} \sum_{L=j-1}^{j+1} \sqrt{2L+1} \, i^L h_L^{\text{in}}(kr) \, C_{L0,1\lambda}^{j\lambda} \boldsymbol{Y}_{jm}^L(\hat{\boldsymbol{r}}) \tag{185}$$

under parity and time reversal. Here we additionally distinguish between incoming and outgoing fields which is crucial for time reversal and important for the S-matrix formalism.

D.1. Parity

We follow the transformation rule mentioned in Appendix C.3 and first consider the transformation of the vector spherical harmonic part [31]

$$I_s \boldsymbol{Y}_{jm}^L(\hat{\boldsymbol{r}}) = -(-1)^L \boldsymbol{Y}_{jm}^L(\hat{\boldsymbol{r}}). \tag{186}$$

Now, with

$$C_{L0,1\lambda}^{j\lambda} = C_{L0,1-\lambda}^{j-\lambda}(-1)^{L+1-j} \tag{187}$$

one gets from Eqs. (183)–(185)

$$I_s \boldsymbol{R}_{jm\lambda}(k, \boldsymbol{r}, t) = (-1)^j \boldsymbol{R}_{jm,-\lambda}(k, \boldsymbol{r}, t) \tag{188}$$

$$I_s \boldsymbol{S}_{jm\lambda}^{\text{in/out}}(k, \boldsymbol{r}, t) = (-1)^j \boldsymbol{S}_{jm,-\lambda}^{\text{in/out}}(k, \boldsymbol{r}, t). \tag{189}$$

D.2. Time reversal

Now, considering the time reversal of the general electromagnetic field discussed in Appendix C.4 we use [31]

$$\boldsymbol{Y}_{jm}^L(\hat{\boldsymbol{r}})^* = (-1)^{L+1+j+m} \boldsymbol{Y}_{j,-m}^L(\hat{\boldsymbol{r}}) \tag{190}$$

to write

$$\left[\sum_{L=j-1}^{j+1} \sqrt{2L+1} \, i^L j_L(kr) \, C_{L0,1\lambda}^{j\lambda} \boldsymbol{Y}_{jm}^L(\hat{\boldsymbol{r}}) \right]^* =$$

$$= \sum_{L=j-1}^{j+1} \sqrt{2L+1} \, (-1)^L i^L j_L(kr) \, C_{L0,1\lambda}^{j\lambda} (-1)^{L+1+j+m} \boldsymbol{Y}_{jm}^L(\hat{\boldsymbol{r}})$$

$$= -(-1)^{j+m} \sum_{L=j-1}^{j+1} \sqrt{2L+1} \, i^L j_L(kr) \, C_{L0,1\lambda}^{j\lambda} \boldsymbol{Y}_{j,-m}^L(\hat{\boldsymbol{r}}) \tag{191}$$

and similarly

$$\left[\sum_{L=j-1}^{j+1} \sqrt{2L+1} \, i^L h_L^{\text{in/out}}(kr) \, C_{L0,1\lambda}^{j\lambda} \boldsymbol{Y}_{jm}^L(\hat{\boldsymbol{r}}) \right]^* =$$

$$= -(-1)^{j+m} \sum_{L=j-1}^{j+1} \sqrt{2L+1} \, i^L h^{\text{out/in}}(kr) \, C_{L0,1\lambda}^{j\lambda} \boldsymbol{Y}_{j,-m}^L(\hat{\boldsymbol{r}}), \tag{192}$$

which for the basis states implies

$$I_t \boldsymbol{R}_{jm\lambda}(k, \boldsymbol{r}, t) = -(-1)^{j+m} \boldsymbol{R}_{j,-m,\lambda}(k, \boldsymbol{r}, t) \tag{193}$$

$$I_t \boldsymbol{S}_{jm\lambda}^{\text{out}}(k, \boldsymbol{r}, t) = -(-1)^{j+m} \boldsymbol{S}_{j,-m,\lambda}^{\text{in}}(k, \boldsymbol{r}, t) \tag{194}$$

$$I_t \boldsymbol{S}_{jm\lambda}^{\text{in}}(k, \boldsymbol{r}, t) = -(-1)^{j+m} \boldsymbol{S}_{j,-m,\lambda}^{\text{out}}(k, \boldsymbol{r}, t). \tag{195}$$

As discussed in Appendix C.4, one should also conjugate the coefficients of the field $f_{jm\lambda}(k)$ when performing time reversal of the total field. We also note that transformations Eqs. (193)–(195) result in an extra minus sign compared to the description with the vector potential in Appendix A.

References

[1] Waterman PC. Matrix formulation of electromagnetic scattering. Proc IEEE 1965;53(8):805–12.

[2] Gouesbet Gérard. T-matrix methods for electromagnetic structured beams: A commented reference database for the period 2014–2018. J Quant Spectrosc Radiat Transfer 2019;230:247–81.

[3] Mishchenko Michael I. Comprehensive thematic T-matrix reference database: a 2017–2019 update. J Quant Spectrosc Radiat Transfer 2020;242:106692.

[4] Theobald Dominik, Egel Amos, Gomard Guillaume, Lemmer Uli. Plane-wave coupling formalism for T-matrix simulations of light scattering by nonspherical particles. Phys Rev A 2017;96:033822.

[5] Egel Amos, Eremin Yuri, Wriedt Thomas, Theobald Dominik, Lemmer Uli, Gomard Guillaume. Extending the applicability of the T-matrix method to light scattering by flat particles on a substrate via truncation of sommerfeld integrals. J Quant Spectrosc Radiat Transfer 2017;202:279–85.

[6] Martin Torleif. T-matrix method for closely adjacent obstacles. J Quant Spectrosc Radiat Transfer 2019;234:40–6.

[7] Schebarchov D, Le Ru EC, Grand J, Auguié B. Mind the gap: testing the Rayleigh hypothesis in T-matrix calculations with adjacent spheroids. Opt Express 2019;27(24):35750–60.

[8] Rother Tom, Hawkins Stuart C. Notes on Rayleigh's hypothesis and the extended boundary condition method. J Acoust Soc Am 2021;149(4):2179–88.

[9] Barkhan J, Ganesh M, Hawkins SC. Approximation of radiating waves in the near-field: Error estimates and application to a class of inverse problems. J Comput Appl Math 2022;401:113769.

[10] Lamprianidis Aristeidis G, Rockstuhl Carsten, Fernandez-Corbaton Ivan. Transcending the Rayleigh hypothesis with multipolar sources distributed across the topological skeleton of a scatterer. J Quant Spectrosc Radiat Transfer 2023;296:108455.

[11] Bech Heinrich, Leder Alfred. Simultaneous determination of particle size and refractive index by time-resolved mie scattering. Optik 2010;121(20):1815–23.

[12] Ambardekar Amol Ashok, Li Yong qing. Optical levitation and manipulation of stuck particles with pulsed optical tweezers. Opt Lett 2005;30(14):1797–9.

[13] Stanciu CD, Hansteen F, Kimel AV, Kirilyuk A, Tsukamoto A, Itoh A, et al. All-optical magnetic recording with circularly polarized light. Phys Rev Lett 2007;99:047601.

[14] Tung Wu-Ki. Group theory in physics. World Scientific; 1985.

[15] Peterson Bo, Ström Staffan. T-matrix for electromagnetic scattering from an arbitrary number of scatterers and representations of E(3). Phys Rev D 1973;8(10):3661.

[16] Wigner E. On unitary representations of the inhomogeneous lorentz group. Ann of Math 1939;40(1):149–204.

[17] Moses Harry E. Photon wave functions and the exact electromagnetic matrix elements for hydrogenic atoms. Phys Rev A 1973;8:1710–21.

[18] Gross Leonard. Norm invariance of mass-zero equations under the conformal group. J Math Phys 1964;5(5):687–95.

[19] Birula Iwo Bialynicki, Birula Zofia Bialynicka. Quantum electrodynamics. Pergamon; 1975.

[20] Fernandez-Corbaton Ivan, Rockstuhl Carsten. Unified theory to describe and engineer conservation laws in light-matter interactions. Phys Rev A 2017;95:053829.

[21] Handapangoda Chintha Chamalie, Premaratne Malin, Pathirana Pubudu N. Plane wave scattering by a spherical di-electric particle in motion: a relativistic extension of the mie theory. Prog Electromag Res-pier 2011;112:349–79.

[22] Garner Timothy J, Lakhtakia Akhlesh, Breakall James K, Bohren Craig F. Time-domain electromagnetic scattering by a sphere in uniform translational motion. J Opt Soc Amer A 2017;34(2):270–9.

[23] Kristensson Gerhard. Scattering of electromagnetic waves by obstacles. In: Electromagnetic waves. Institution of Engineering and Technology; 2016.

[24] Martin PA. Time-domain scattering. In: Encyclopedia of mathematics and its applications. Cambridge University Press; 2021.

[25] Beutel Dominik, Groner Achim, Rockstuhl Carsten, Fernandez-Corbaton Ivan. Efficient simulation of biperiodic, layered structures based on the T-matrix method. J Opt Soc Amer B 2021;38(6):1782–91.

[26] Beutel Dominik, Fernandez-Corbaton Ivan, Rockstuhl Carsten. Unified lattice sums accommodating multiple sublattices for solutions of the helmholtz equation in two and three dimensions. Phys Rev A 2023;107:013508.

[27] Ganesh M, Hawkins SC. Three dimensional electromagnetic scattering T-matrix computations. J Comput Appl Math 2010;234(6):1702–9, Eighth International Conference on Mathematical and Numerical Aspects of Waves (Waves 2007).

[28] Petrov Dmitry, Shkuratov Yuriy, Videen Gorden. Electromagnetic wave scattering from particles of arbitrary shapes. J Quant Spectrosc Radiat Transfer 2011;112(11):1636–45, Electromagnetic and Light Scattering by Nonspherical Particles XII.

[29] Petrov Dmitry, Shkuratov Yuriy, Videen Gorden. Light scattering by arbitrary shaped particles with rough surfaces: Sh-matrices approach. J Quant Spectrosc Radiat Transfer 2012;113(18):2406–18, Electromagnetic and Light Scattering by non-spherical particles XIII.

[30] Fruhnert Martin, Fernandez-Corbaton Ivan, Yannopapas Vassilios, Rockstuhl Carsten. Computing the T-matrix of a scattering object with multiple plane wave illuminations. Beilstein J Nanotechnol 2017;8:614–26.

[31] Varshalovich DA, Moskalev AN, Khersonskii VK. Quantum theory of angular momentum. WORLD SCIENTIFIC; 1988.

[32] Weinberg Steven. The quantum theory of fields. 1st ed. vol. 1, Cambridge University Press; 1995.

[33] Zeldovich YaB. Number of quanta as an invariant of the classical electromagnetic field. Dokl Acad Sci USSR 1965;163:1359, [in Russian].

[34] Bateman H. The conformal transformations of a space of four dimensions and their applications to geometrical optics. In: Proceedings of the London mathematical society. s2-7, (1):1909, p. 70–89.

[35] Jackson John David. Classical electrodynamics. New York: Wiley; 1998.

[36] Moses HE. Transformation from a linear momentum to an angular momentum basis for particles of zero mass and finite spin. J Math Phys 1965;6(6):928–40.

[37] Santiago X Garcia, Hammerschmidt M, Burger S, Rockstuhl C, Fernandez-Corbaton I, Zschiedrich L. Decomposition of scattered electromagnetic fields into vector spherical wave functions on surfaces with general shapes. Phys Rev B 2019;99:045406.

[38] Wittmann RC. Spherical wave operators and the translation formulas. IEEE Trans Antennas and Propagation 1988;36(8):1078–87.

[39] Colton David, Kress Rainer. Inverse acoustic and electromagnetic scattering theory. vol. 93, New York: Springer Science & Business Media; 2012.

[40] Mishchenko Michael I, Travis Larry D, Lacis Andrew A. Scattering, absorption, and emission of light by small particles. Cambridge University Press; 2002.

[41] Palik Edward D. Handbook of optical constants of solids. Academic Press; 1998.

[42] du Preez-Wilkinson Nathaniel, Stilgoe Alexander B, Alzaidi Thuraya, Rubinsztein-Dunlop Halina, Nieminen Timo A. Forces due to pulsed beams in optical tweezers: linear effects. Opt Express 2015;23(6):7190–208.

[43] Cohen-Tannoudji Claude, Dupont-Roc Jacques, Grynberg Gilbert. Photons and atoms: Introduction to quantum electrodynamics. Wiley; 1989.